Award Number: W81XWH-09-1-0667

TITLE: "Investigating the Role of Indoleamine 2,3- dioxygenase (IDO) in Breast Cancer Metastasis"

PRINCIPAL INVESTIGATOR: Courtney Smith, Ph.D.

CONTRACTING ORGANIZATION: Lankenau Institute for Medical Research
Wynnewood, PA 19096

REPORT DATE: September 2012

TYPE OF REPORT: Final

PREPARED FOR: U.S. Army Medical Research and Materiel Command
Fort Detrick, Maryland 21702-5012

REPORT DOCUMENTATION PAGE

Form Approved
OMB No. 0704-0188

1. REPORT DATE	2. REPORT TYPE	3. DATES COVERED
1 September 2012	Final	1 Sep 2009 – 31 Aug 2012

4. TITLE AND SUBTITLE

Investigating the Role of Indoleamine 2,3-Dioxygenase (IDO) in Breast Cancer Metastasis

5a. CONTRACT NUMBER

5b. GRANT NUMBER
W81XWH-09-1-0667

5c. PROGRAM ELEMENT NUMBER

6. AUTHOR(S)
Courtney Smith, Ph.D.

E-Mail: SmithCo@mlhs.org

5d. PROJECT NUMBER

5e. TASK NUMBER

5f. WORK UNIT NUMBER

7. PERFORMING ORGANIZATION NAME(S) AND ADDRESS(ES)

Lankenau Institute for Medical Research

Wynnewood, PA 19096

8. PERFORMING ORGANIZATION REPORT NUMBER

9. SPONSORING / MONITORING AGENCY NAME(S) AND ADDRESS(ES)
U.S. Army Medical Research and Materiel Command
Fort Detrick, Maryland 21702-5012

10. SPONSOR/MONITOR'S ACRONYM(S)

11. SPONSOR/MONITOR'S REPORT NUMBER(S)

12. DISTRIBUTION / AVAILABILITY STATEMENT
Approved for Public Release; Distribution Unlimited

13. SUPPLEMENTARY NOTES

14. ABSTRACT
First identified as a mediator of acquired immune tolerance of the 'foreign' fetus from maternal immunity, the tryptophan-catabolizing enzyme IDO (indoleamine 2,3-dioxygenase) has since been implicated in tumor escape from the host immune system. Primary tumor growth of the metastatic 4T1 breast cancer model was unaffected in the IDO-deficient mice, however, survival was significantly improved. This provided a basis for our studies exploring the importance of IDO in the metastatic site of the lung. Elevation of the inflammatory cytokine IL-6 was associated with tumor outgrowth in the lungs but was greatly attenuated with the loss of IDO, consistent with the in vitro demonstration that IDO activity markedly potentiates IL-6 production. MDSCs (myeloid derived suppressor cells) exhibited reduced T-cell suppressive activity when isolated from tumor-bearing, IDO-deficient animals that could be rescued by ectopic production of IL-6 in the tumor. IL-6 production could likewise reverse the pulmonary metastasis resistance exhibited by IDO-deficient mice. Interestingly, while there is a clear role of the immune system in lung tumor and metastatic outgrowth, IDO-deficient mice appear to have reduced vascularization in the lung which may partly contribute to reduced tumor formation. Together, these findings genetically validate IDO as a therapeutic target in the settings of metastasis and establish the importance of IDO as a driver of IL-6 production and MDSC function. Furthermore, the correlation of IDO to angiogenesis may be a new insight into the role of this enzyme in cancer.

15. SUBJECT TERMS
indoleamine 2,3-dioxygenase, lung metastasis, vascularization, IL-6, myeloid derived suppressor cells, 4T1

16. SECURITY CLASSIFICATION OF:			17. LIMITATION OF ABSTRACT	18. NUMBER OF PAGES	19a. NAME OF RESPONSIBLE PERSON
a. REPORT	b. ABSTRACT	c. THIS PAGE			USAMRMC
U	U	U	UU	47	19b. TELEPHONE NUMBER *(include area code)*

Table of Contents

Page

INTRODUCTION:

Treatment of cancer commonly entails surgical resection followed by chemotherapy and radiotherapy, a regimen that results in variable degrees of long-term success. This is in part due to the ability of tumor cells to escape these methods of treatment and restore primary tumor growth and, more importantly, distant metastasis. The majority of cancer related deaths are due to the development of metastatic disease as opposed to primary tumor burden. In human breast cancer, the lungs are the primary site of metastasis followed by bone (1,2). Evidence of metastasis in breast cancer patients is considered a strong negative prognostic factor. Therefore, advances in treatment to reduce metastasis will greatly improve survival in breast cancer.

The finding that there is a synergistic benefit to combining chemotherapy with the indoleamine-2,3-dioxygenase (IDO1) inhibitor 1-methyl-tryptophan (1MT) in preclinical mouse models of breast cancer, (3) suggests a promising new therapeutic approach. IDO1 is the rate-limiting factor in tryptophan catabolism; however, it is not involved in dietary catabolism in the liver, leading researchers to determine an alternative role for this enzyme. The seminal demonstration that 1MT could elicit MHC-restricted T cell-mediated rejection of allogeneic mouse concepti (4,5) established a role for IDO1 in mediating immune tolerance. Studies have also revealed a pathophysiological link between IDO1 and cancer with increased levels of IDO1 activity being associated with a variety of different tumors (6,7). The therapeutic potential of targeting IDO1 in conjunction with chemotherapy has been demonstrated in the MMTV-Neu mouse model of breast cancer. The effects of 1MT were found to be greatly enhanced when given in conjunction with the commonly used chemotherapeutic agent paclitaxel (3). Depletion of either CD4+ or CD8+ T-cells in these mice abolished the benefit provided by 1MT indicating the importance of T cell immunity in the antitumor response.

The immunosuppressive function of IDO1 manifests in several manners. Collectively, IDO1 and its metabolites can directly suppress T cells (17-20) and NK cells (21) as well as enhance local Tregs (22). While there are studies showing the protumorigenic capabilities of myeloid derived suppressor cells (MDSCs) (13-16), our publication is the first to show that this population is also be affected by IDO1. Furthermore, IDO1 is produced in response to IFN-γ, an important cytokine modulator of inflammation. It is therefore reasonable to hypothesize that IDO1 not only regulates immune cells but may be regulated by or may regulate cytokine production in the host, resulting in a protumorigenic microenvironment.

To address these questions, we have characterized tumorigenesis in *Ido1-/-* mice to allow for the study of IDO1 in metastasis. Using an immune competent model, we focused on the role of IDO1 in the immune response to tumors. We have selected the highly metastatic 4T1 breast cancer model which progresses similarly to human breast cancer (10,12). Using this model, we were able to compare the metastatic sites of *Ido1-/-* and WT mice and evaluate the importance of IDO1 in metastatic outgrowth. Our studies in this model demonstrate that the loss of IDO1 improves survival due to reduced pulmonary metastasis through the reduced immunosuppressive response of the host.

BODY:

Prior to commencement of all animal-related experiments, IACUC approval to conduct the proposed experiments was obtained. In our **first specific aim,** we proposed to evaluate IDO1 activity in the lungs of 4T1 tumor-bearing mice and determine the source of its expression. 4T1 cells were orthotopically injected into the mammary fatpad of BALB/c and *Ido1-/-* mice. After two weeks, palpable tumors were observed and two perpendicular measurements were taken at weekly intervals over a six week period to evaluate primary tumor growth. Initial experiments were performed using a 4T1-derived cell line expressing luciferase (4T1-luc) as we anticipated visualization of metastasis using bioluminescence. However, during our experiments, we found that the luciferase was downregulated in the metastatic cells; whether this reflects the inherent nature of metastatic cells or if it is a result of immune system evasion following intravasation was not investigated. Regardless, the use of the luciferase 4T1 line was deemed unnecessary as the level of bioluminescence underrepresented the amount of metastatic tumor cells. Once we established that the 4T1 luciferase line was no longer necessary, we repeated our results using the parental 4T1 cell line. Both cell lines showed that primary tumors in *Ido1-/-* mice exhibited a similar growth rate to that observed in the wild-type control **(Fig. 1 A-B).** However, survival was increased significantly in *Ido1-/-* hosts compared with WT hosts after challenge with either a 4T1-luciferase–expressing subclone or with parental 4T1 cells, despite an overall shift in the curves **(Fig. 1 C-D).**

The 4T1 model is a well characterized system to replicate stage IV breast cancer due to the spontaneous metastasis to lungs, liver, lymph node and brain. The highly metastatic nature of 4T1 suggested that the difference in survival, while not related to primary tumor burden, may be a result of disproportionate metastatic burden. Therefore, lung, liver and brain were harvested along with blood and analyzed by the clonogenic assay for metastatic tumors. Metastatic colonies in the brain and liver did not exceed ten per organ and had no statistical difference between WT and *Ido1-/-* mice (**Fig. 2A-B**). Interestingly, metastatic colonies in the lung showed that there was less metastatic burden in the lungs of *Ido1-/-* mice by approximately 10-fold (**Fig. 2C**). Serum isolated from *Ido1-/-* and wild-type controls showed similar levels of metastatic cells, indicating that the reduced metastatic spread is not due to decreased tumor cell migration but rather to the reduced ability to establish tumor metastases (**Fig. 2C**). The observation in lung was further confirmed using both India Ink re-inflation of the lungs and microCT (**Fig. 2E**). Injection of India Ink into the lungs allowed normal lung tissue to absorb the stain causing metastatic regions to be visualized as white nodules. Similarly, microCT showed normal lung as a dark region while the significantly denser metastatic regions appeared white, further confirming that the improved survival of *Ido1-/-* mice was due to reduced pulmonary metastasis. Because excision of the primary tumor can alter immune-based effects on metastasis (30), we evaluated the metastatic burden in resected mice. *Ido1-/-* mice continued to exhibit significant resistance to metastasis development **(Fig. 2D)**, indicating that IDO-mediated support of metastatic development in the lung was not dependent on the presence of the primary tumor. As proposed in the statement of work, these experiments were completed in the first year and a repeat performed in the second year to confirm the original observations. The second study showed the same pattern of reduced metastatic burden and increased survival in *Ido1-/-* mice providing a final n-value of greater than 20 mice per group. Additionally, in the second year, a smaller cohort of mice injected with parental 4T1 cells were used to negate the possibility that the presence of luciferase affected this study.

The reduction in metastasis observed in the *Ido1-/-* mice suggested that IDO1 is pro-metastatic. We therefore investigated the presence of IDO1 protein in the microenvironment of the lung. Time points were collected at one week intervals from two to six weeks for WT and two to eight weeks for *Ido1-/-* mice. Baseline levels were obtained from non-tumor-bearing mice. In WT mice, early metastases were observed at approximately three to four weeks. By five weeks, there was a substantial metastatic burden, leading to a lethal burden in week six. By comparison, these timepoints were shifted two weeks later for *Ido1-/-* mice requiring timepoints in *Ido1-/-* mice to be extended to eight weeks. No data at seven and eight weeks was available for WT mice as they did not survive past six weeks. Protein IDO1 was measured by immunoprecipitation with αIDO1 and Western blot with a second IDO1 antibody. As expected, *Ido1-/-* mice did not express any IDO1 protein, however, WT mice had greater levels of IDO1 as metastatic burden increased (**Fig. 3A**). Using LC/MS/MS to measure the presence of kynurenine, a product of tryptophan catabolism by IDO1, we were able to demonstrate that the IDO1 protein in the lung microenvironment was functionally active, and the level of kynurenine increased directly in relation to the protein (**Fig. 3B**). This further supported the importance of IDO1 in the lungs for optimal conditions of metastatic outgrowth. These data were collected in a second cohort of mice in year two to increase the n-value to greater than ten mice per group. The data from these figures is presented in our appended Cancer Discovery paper. Cancer Discovery is the flagship journal from AACR that, while still a young journal, has received the prodigious 2011 American Publishers Award for Professional and Scholarly Excellence and is acknowledged as publishing top-rated peer reviewed articles.

Current roadblocks remain in the difficulty of obtaining an IDO1 antibody suitable for immunohistochemistry. Until recently, existing antibodies have not been used on *Ido1-/-* mice and therefore no publications of IDO1 immunohistochemistry have this control. Our lab and others have observed high levels of non-specific staining in *Ido1-/-* samples, suggesting that these antibodies are not suitable for IHC. We are currently collaborating with other researchers at LIMR to develop our own antibody to IDO1. Our previous attempts to generate an antibody against full length protein have been unsuccessful. Therefore, we are now generating antibodies to an IDO peptide located in the deleted region of the *Ido1-/-* mice. These studies are currently underway.

Despite the inability to detect IDO1 by immunohistochemistry, we worked out conditions for staining and discovered an interesting result surrounding the *Ido1-/-* mice. While optimizing the Blood Vessel Staining Kit from Millipore to look for CD31 and von Willebrand's as proposed in the first aim, we costained with caveolin-1 (cav-1), another marker for blood vessels. The conditions for staining Cav-1 had previously been optimized for immunofluorescence. While we initially were interested in the level of Cav-1 in the metastatic lung, we noticed that there was a difference in the normal controls (**Fig. 4C**). Immunofluorescent staining of Cav-1 revealed that there are fewer pulmonary vessels in *Ido1-/-* animals by approximately 1.6-fold (**Fig. 4**). Further analysis of vessel size indicated that there was little difference in the number of large vessels but rather the level of small- to medium-sized vessels had the most dramatic difference (**Fig. 4B,D)**. This was confirmed after analysis using the microCT to analyze previously collected images (**Fig. 4A)** (additional supplemental videos can be viewed in the Cancer Discovery publication). This discovery may provide an important new function for IDO in metastasis.

The **second specific aim** was designed to characterize the immune response in the lungs of 4T1 tumor-bearing mice. During the second year, we performed bone marrow chimera experiments. To effectively determine the reconstitution of the irradiated mice, we proposed the use of C.B-17 mice. C.B-17 mice are a congenic strain on a BALB/c background that carries the immunoglobulin heavy chain allele (Igh-1b) found on C57BL6 mice. This provides a marker to determine the level of reconstitution. Our pilot run showed that we have greater than 99% successful reconstitution in our mice. Furthermore we found that the use of C.B-17 mice in place of BALB/c did not affect the rate of lung metastasis as determined by the number of circulating tumor cells and number of pulmonary metastases counted by the colony forming assay **(Fig. 5A)**.

Following the initial pilot experiment, we set up two bone marrow chimera experiments to measure the effects of the immune cells. The first experiment was set up as a clonogenic colony forming assay (**Fig. 5B**) and the second as a survival study (**Fig. 5C**). Both experiments resulted in greater metastasis susceptibility of mice with *Ido1-/-* marrow transplanted into an irradiated *Ido1-/-* mouse compared to irradiated WT mice receiving WT bone marrow. As these served as our control groups and the data runs counter to our expected results, we were unable to interpret the experimental conditions of transplanting WT mice with *Ido1-/-* marrow and visa versa. Due to both experiments resulting in the same outcome, we must consider the possibility that *Ido1-/-* mice are more susceptible to metastasis as a result of irradiation.

While data from the bone marrow chimera experiments were inconclusive, we proceeded to determine which immune cells may be involved in metastasis by focusing on the infiltrating immune cell profile. The profile was evaluated for differences between the WT and *Ido1-/-* 4T1 tumor-bearing mice by enzymatically dissociating lung tissue to form single cell suspensions for analysis by flow cytometry using the following panel of antibodies: αCD45, αCD4, αCD8, αCD3, αB220, αCD11c, αCD11b and αGr1 **(Fig. 6)**. Lung samples were collected at one week intervals between one and five weeks following tumor engraftment (**Fig. 6A-E**). Between two and three weeks, the immunosuppressive MDSC population, identified here as CD11b+Gr1+, was greatly increased in the WT mice (**Fig. 6F**). The data collected from these studies represent the percentage of positive cells from each immune cell population out of the entire CD4+ population. The data indicated greater numbers of MDSCs in WT mice. These data parallel previous data in IL-1β knockout mice that showed the same delay in MDSC accumulation (4).

In response to reviewer comments on our manuscript, we provided further supplemental data of the functional effects on MDSCs. In collaboration with the laboratory of Dr. Suzanne Ostrand-Rosenberg, we demonstrated that MDSC-suppressive activity is attenuated in IDO-deficient mice. MDSCs from WT and *Ido1-/-* mice did not have phenotypic differences based on microscopic evaluation of these cells using hematoxylin and eosin staining (**Fig 7A).** However, the functional ability to suppress T cells was impaired in MDSCs from these mice as they were less able to suppress both CD4+ and CD8+ T-cells **(Fig. 7B-C).** Detailed explanations and supplemental information for MDSC phenotyping can be found in the appended Cancer Discovery supplemental figure 3.

The microenvironment of the lung affects the ability of 4T1 tumors to metastasize. Loss of IDO1 reduces tumor metastasis and is accompanied by a shift in the immune cell profile, implicating the immune system in this suppression. Additionally, environmental cues may be altered such that tumor growth is not favored. Due to studies implicating a relationship between cytokines and IDO1, we hypothesized in **the third specific aim** that the cytokine profile in the lungs of tumor-bearing mice in the *Ido1-/-* versus the wild-type would be different.

Lung homogenates were evaluated using the Cytometric Bead Array (BD Biosciences) from samples collected at one week intervals from two to five weeks following tumor engraftment from groups of at least four mice each. This array uses amplified fluorescence detection by flow cytometry to detect soluble analytes to provide multiplexed data comparable to a classical ELISA. Initially, lung homogenates were analyzed for a set of cytokines that included IL-2, IL-4, IL-5 and IL-17 to determine differences in cytokines influencing immune cell maturation. Specifically, these cytokines regulate divergence into Th1, Th2 or Th17 cell lineages. It is generally accepted that a Th1 environment suppresses tumor outgrowth while a Th2 environment promotes immune escape. The cytokine profile for Th1/Th2/Th17 showed no measurable levels of these cytokines above the limit of detection (**Fig. 8)**.

This prompted the use of a second panel of cytokines that reflect inflammation in the lung and included IL-6, IL-10, MCP-1, IFN-γ, TNF and IL-12p70. Samples were collected and analyzed similarly to the Th1/Th2/Th17 analysis. MCP-1 and IL-6 showed increased levels during tumor progression in WT mice (**Fig. 9A-B**). MCP-1 showed higher levels of expression in WT mice starting at two weeks and continuing through six weeks (**Fig. 9A**). The increase was on average two-fold greater than the *Ido1-/-* mice. While MCP-1 was increased in *Ido1-/-* mice, the response was less robust. Similar data was acquired for IL-6 with the difference that increased IL-6 was not observed until four weeks after orthotopic injection at which time there was a two-fold increase (**Fig. 9B**). At five weeks, IL-6 was on average four-fold higher than the *Ido1-/-* mice which only had a marginal rise in IL-6 levels. These results collectively demonstrated that *Ido1-/-* mice have a suppressed inflammatory response to 4T1. Both TNF and IFN-γ showed equal elevations at each time point between WT and *Ido1-/-* starting at three weeks and continuing through six weeks (**Fig. 9C-D**). These cytokines are generalized responders to inflammation and may reflect a response to the primary tumor burden or early tumor cell extravasation. There was no upregulation of IL-12p70 or IL-10 in either WT or *Ido1-/-* mice (**Fig. 9E-F**).

After identifying IL-6 as a cytokine involved in establishing metastatic progression, we wanted to demonstrate a direct connection with IDO. Due to the difficulty in studying a mouse model, we invoked a cell culture system to provide a clear mechanism to study IDO and IL-6. Using lipopolysaccharide (LPS) to induce IDO activity in the monocytic U937 cells, we observed induction of IL-6 (**Fig. 10A).** The addition of a competitive IDO-inhibitory compound, MTH-tryptophan, significantly suppressed the observed increase in both IDO activity as well as IL-6 production **(Fig. 10B)**. The effect was confirmed in a second monocytic cell line HL-60 (**Fig. 10C)**. Using HL-60 cells, we successfully knocked down IDO using siRNA-mediated interference (reduced to 90%) and found that IL-6 induction was suppressed (**Fig. 10C)**. These data supported our *in vivo* studies connecting IDO activity to the elevated production of IL-6.

To connect IL-6 to MDSC activity *in vivo*, we generated an IL-6 overexpressing 4T1 cell line (4T1-IL-6). Parental 4T1 or the 4T1-IL6 cells were orthotopically injected into WT or *Ido1-/-* mice. Due to the high levels of IL6 in the primary tumors, the mice succumbed to the primary tumor effects and not pulmonary metastases. We therefore intravenously engrafted both cell lines into WT and *Ido1-/-* mice and found that the *Ido1-/-* mice maintained their resistance to pulmonary metastasis formation (tumor burden was 30.4-fold and 31.6-fold lower in *Ido1-/-* versus WT mice challenged with 4T1 and 4T1-IL6 cells, respectively (**Fig. 11A**). The metastatic burden in the 4T1-IL6 challenged mice was proportionally increased, indicating that IL-6 is not being produced at saturating levels in the 4T1 injected WT animals. However, comparison of metastatic burden in WT mice injected with parental 4T1 and *Ido1-/-* mice injected with 4T1-IL6

showed only a 4.8-fold differential. Thus, IL-6 supplementation restored susceptibility of *Ido1-/-* mice to pulmonary metastasis development. This also paralleled the effects of the MDSC function from these groups as well (**Fig. 11B**). While MDSC function was restored proportionally in WT and *Ido1-/-* mice with 4T1-IL6 over their 4T1 parental counterparts, the 4T1-IL6 tumor challenged *Ido1-/-* mice had MDSCs that were functionally like the 4T1 tumor challenged WT mice. IL-6 and MDSC data can also been viewed in the appended Cancer Discovery publication.

KEY RESEARCH ACCOMPLISHMENTS:

- Found that the improved survival of *Ido1-/-* mice is due to reduced pulmonary metastasis
- Confirmed that expression of IDO1 protein is present in the metastatic site of the lung in the orthotopically engrafted 4T1 breast cancer model and correlated with activity as evidenced by increased kynurenine production
- Demonstrated that equal numbers of circulating tumor cells are observed in WT and *Ido1-/-* mice suggesting the effect of IDO1 loss and improved survival is due to a decreased adherence, extravasation or metastatic outgrowth
- Determined that the immunosuppressive MDSC population increases more rapidly in WT mice compared to *Ido1-/-*, a pattern previously seen in IL-1β knockout mice; further showed a functional defect in MDSC function in *Ido1-/-* mice
- Found measureable differences in inflammatory cytokine levels between *Ido1-/-* mice and the WT counterparts, particularly pertaining to the cytokines IL-6 and MCP-1
- Demonstrated in culture that IDO inhibitors can block production of IL-6 in response to LPS induction and IDO-inhibitory compound MTH-tryptophan
- Overexpressed IL-6 in 4T1 cells to demonstrate that metastatic potential can be restored in *Ido1-/-* mice to WT levels
- Implicated IDO in the reduced vascularization of normal lung

REPORTABLE OUTCOMES:

PUBLICATIONS

1. **Smith, C.,** Chang, M.Y., Parker, K., Beury, D., DuHadaway, J., Flick, H., Boulden, J., Sutanto-Ward, E., Soler, A.J., Laury-Kleintop, L., Mandik-Nayak, L., Metz, R., Ostrand-Rosenberg, S., Prendergast, G.C., Muller, A.J. 2012. IDO is a nodal pathogenic driver of lung cancer and metastasis development. Cancer Discov. **2**: 1-14.

2. **Smith, C.,** Prendergast, G.C., Muller A.J. "IDO pathway: Inflammation and Immune Escape". Cancer Immunotherapy. 2nd ed. Ed. George Prendergast and Elizabeth Jaffee. New York: Elsevier, 2012, in production. Print.

3. Prendergast, G.C., Metz, R., Chang, M.Y., **Smith, C.,** Muller, A.J., Ostrand-Rosenberg, S. "Indoleamine 2,3-dioxygenase amino acid metabolism and tumor-associated macrophages:

regulation in cancer-associated inflammation and immune escape." Tumor-Associated Macrophages. Ed. Toby Lawrence and Thorsten Hagemann. New York: Springer, 2012, 91-104. Print.

4. Chang, M.Y., **Smith, C.,** Duhadaway, J.B., Pyle, J.R., Boulden, J., Soler, A.P., Muller, A.J., Laury-Kleintop, L.D., Prendergast, G.C. 2011. Cardiac and gastrointestinal liabilities caused by deficiency in the immune modulatory enzyme indoleamine 2,3-dioxygenase. Cancer Biol. Ther. 12: 1050-1058.

5. **Smith, C.,** Prendergast, G.C., Muller A.J. "IDO pathway: Inflammation and Immune Escape". Cancer Immunotherapy. 2nd ed. Ed. George Prendergast and Elizabeth Jaffee. New York: Elsevier, 2012, in production. Print.

MEETINGS

1. **Smith, C.** Indoleamine 2,3-dioxygenase (IDO) supports metastatic outgrowth of the 4T1 breast cancer mouse model. Keystone Symposia on Molecular and Cellular Biology of Immune Escape in Cancer. Keystone, Colorado. February 7-12, 2010. Invited Speaker.

   Travel Award/Conference Assistant for Keystone Symposium on Molecular and Cellular Biology of Immune Escape in Cancer, Feb 7-12, 2010, Keystone Resort, Keystone, CO

2. **Smith, C.,** Duhadaway, J., Muller, A.J., Prendergast, G.C. Indoleamine 2,3-dioxygenase (IDO) supports metastatic outgrowth of the 4T1 breast cancer mouse model. Keystone Symposia on Molecular and Cellular Biology of Immune Escape in Cancer. Keystone, Colorado. February 7-12, 2010. Poster Presentation.

3. **Smith, C.,** Duhadaway, J., Muller, A.J., Prendergast, G.C. Indoleamine 2,3-dioxygenase (IDO) supports metastatic outgrowth of the 4T1 breast cancer mouse model. AACR Joint Conference on Metastasis and the Tumor Microenvironment. Philadelphia, PA. September 12-15, 2010. Poster Presentation.

4. **Smith, C.,** Chang, M-Y., Flick, H., DuHadaway, J., Mandik-Nayak, L., Laury-Kleintop, L., Parker, K., Beury, D., Ostrand-Rosenberg, S., Prendergast, G.C., Muller, A.J. IDO drives tumor-promoting, pathogenic inflammation in lung. AACR Annual Meeting. Chicago, IL. March 31-April 4, 2012.Poster Presentation.

PERSONNEL:

Courtney Smith

CONCLUSION:

There are over 40,000 deaths each year in the US resulting from the metastatic spread of breast cancer. Based on data from our lab and others, an IND (investigational new drug) application for the IDO1 inhibitor D-1MT was approved and Phase I clinical trials have commenced. Breast cancer is identified in the clinical development plan as one of the high priority disease indications for evaluation in Phase IIA studies that will be used to determine the clinical scenarios best suited for the Phase II/III clinical development of this agent. Our recently published finding that D-1MT treatment in combination with cyclophosphamide chemotherapy significantly improved survival in mice bearing highly malignant 4T1 tumors (9) suggests for the first time that this approach may be applicable to metastatic disease as well.

Using the IDO1-knockout mouse strain, we have been able to genetically establish that IDO1 is important for supporting the development of pulmonary metastases from orthotopic 4T1 tumors. The core goal of the proposed project has been to determine the underlying biological basis for this pro-metastatic effect of IDO1. The data collected from these experiments resulted in the first publication that IDO affects MDSC function by making them less able to suppress both CD4+ and CD8+ T-cells. The high levels of IL-6 and MCP-1 in the metastatic lungs of WT mice further support the role of the IDO in immune system regulation. The presence of IL-6 was correlated with increased metastasis in WT mice while *Ido1-/-* mice had low levels of IL-6 and less metastasis. To directly tie IDO to IL-6 production, we utilized two cell lines that were induced with LPS to produce IDO. This induction resulted in IL-6 production and the addition of an IDO-inhibitor reduced both IDO levels and IL-6. *In vivo,* we have shown that IDO deficiency not only affects IL-6-dependent, MDSC driven immune escape but also lung vascularization. While models of exogenous IDO overexpression in tumor xenografts have shown enhanced tumor vascularization (26, 27), these studies genetically establish a role for IDO in supporting vascular development under native physiological conditions. The reduced numbers of vessels in IDO1 deficient mice suggest that IDO supports the metastatic dissemination into lung tissue where IDO can readily and significantly be induced during tumor initiation. Future experiments investigating the connection between IDO and vascularization will be critical in understand this cancer target.

The data produced from these studies have elucidated a novel mechanism of action through which IDO1 inhibitors can enhance the antitumor immune response achieved with cyclophosphamide chemotherapy, a frontline agent for the treatment of breast cancer patients. The results of these studies could have immediate bearing on how future clinical trials with IDO1 inhibitory compounds are designed and may lead to the development of more effective strategies for administering IDO1 inhibitors for the treatment of patients with metastatic breast cancer.

REFERENCES:

1) (1994). "Impact of follow-up testing on survival and health-related quality of life in breast cancer patients. A multicenter randomized controlled trial. The GIVIO Investigators." Jama 271(20): 1587-92.

2) Rosselli Del Turco, M., D. Palli, et al. (1994). "Intensive diagnostic follow-up after treatment of primary breast cancer. A randomized trial. National Research Council Project on Breast Cancer follow-up." Jama 271(20): 1593-7.

3) Muller, A. J., J. B. DuHadaway, et al. (2005). "Inhibition of indoleamine 2,3-dioxygenase, an immunoregulatory target of the cancer suppression gene Bin1, potentiates cancer chemotherapy." Nat Med 11(3): 312-9.

4) Mellor, A. L., J. Sivakumar, et al. (2001). "Prevention of T cell-driven complement activation and inflammation by tryptophan catabolism during pregnancy." Nat Immunol 2(1): 64-8.

5) Munn, D. H., M. Zhou, et al. (1998). "Prevention of allogeneic fetal rejection by tryptophan catabolism." Science 281(5380): 1191-3.

6) Brandacher, G., A. Perathoner, et al. (2006). "Prognostic value of indoleamine 2,3-dioxygenase expression in colorectal cancer: effect on tumor-infiltrating T cells." Clin Cancer Res 12(4): 1144-51.

7) Okamoto, A., T. Nikaido, et al. (2005). "Indoleamine 2,3-dioxygenase serves as a marker of poor prognosis in gene expression profiles of serous ovarian cancer cells." Clin Cancer Res 11(16): 6030-9.

8) Munn, D. H., M. D. Sharma, et al. (2004). "Expression of indoleamine 2,3-dioxygenase by plasmacytoid dendritic cells in tumor-draining lymph nodes." J Clin Invest 114(2): 280-90.

9) Hou, D. Y., A. J. Muller, et al. (2007). "Inhibition of indoleamine 2,3-dioxygenase in dendritic cells by stereoisomers of 1-methyl-tryptophan correlates with antitumor responses." Cancer Res 67(2): 792-801.

10) Pulaski BA, Ostrand-Rosenberg S. Mouse 4T1 breast tumor model. In: Coligan JE, Kruisbeek AM, Margulies DH, Shevach EM, Strober W, editors. Current protocols in immunology, Vol. 4. New York: John Wiley; 2001. p. 20.2.1.

11) Aslakson C, Miller F. Selective events in the metastatic process defined by analysis of the sequential dissemination of subpopulations of a mouse mammary tumor. Cancer Res 1992;52:1399 –1405.

12) Miller F, Miller B, Heppner G. Characterization of metastatic heterogeneity among subpopulations of a single mouse mammary tumor: heterogeneity in phenotypic stability. Invasion Metastasis 1983;3:22–31.

13) Gabrilovich D. Mechanisms and functional significance of tumour-induced dendritic-cell defects. Nat Rev Immunol 2004;4:941–52.

14) Serafini P, Borrello I, Bronte V. Myeloid suppressor cells in cancer: recruitment, phenotype, properties, and mechanisms of immune suppression. Semin Cancer Biol 2006;16:53–65.

15) Rodriguez PC, Ochoa AC. T cell dysfunction in cancer: role of myeloid cells and tumor cells regulating amino acid availability and oxidative stress. Semin Cancer Biol 2006;16:66–72.

16) Sinha P, Clements VK, Miller S, Ostrand-Rosenberg S. Tumor immunity: a balancing act between T cell activation, macrophage activation and tumor-induced immune suppression. Cancer Immunol Immunother 2005;54:1137–42.

17) Fallarino, F., et al. 2002. T cell apoptosis by tryptophan catabolism. *Cell Death Differ.* **9**:1069–1077.

18) Frumento, G., et al. 2002. Tryptophan-derived catabolites are responsible for inhibition of T and natural killer cell proliferation induced by indoleamine 2,3-dioxygenase. *J. Exp. Med.* **196**:459–468.

19) Terness, P., et al. 2002. Inhibition of allogeneic T cell proliferation by indoleamine 2,3-dioxygenase-expressing dendritic cells: mediation of suppression by tryptophan metabolites. *J. Exp. Med.* **196**:447–457.

20) Weber, W.P., et al. 2006. Differential effects of the tryptophan metabolite 3-hydroxyanthranilic acid on the proliferation of human CD8+ T cells induced by TCR triggering or homeostatic cytokines. *Eur. J. Immunol.* **36**:296–304.

21) Chiesa, M.D., et al. 2006. The tryptophan cataboliteL-kynurenine inhibits the surface expression of NKp46- and NKG2D-activating receptors and regulates NK-cell function. *Blood.* **108**:4118–4125.

22) Fallarino, F., et al. 2003. Modulation of tryptophan catabolism by regulatory T cells. *Nat. Immunol.* **4**:1206–1212.

23) Källberg E., et al. 2010. Indoleamine 2,3-dioxygenase (IDO) activity influence tumor growth in the TRAMP prostate cancer model. *Prostate*. **70:**1461-70.

24) Bunt, S.K, et al. 2007. Reduced inflammation in the tumor microenvironment delays the accumulation of myeloid-derived suppressor cells and limits tumor progression. *Cancer Res.* **67:**10019-10026.

25) Jackson EL, Willis N, Mercer K, Bronson RT, Crowley D, Montoya R, et al. Analysis of lung tumor initiation and progression using conditional expression of oncogenic K-ras. Genes Dev 2001;15:3243–8.

26) Nonaka H, Saga Y, Fujiwara H, Akimoto H, Yamada A, Kagawa S, et al. Indoleamine 2,3-dioxygenase promotes peritoneal dissemination of ovarian cancer through inhibition of natural killer cell function and angiogenesis promotion. Int J Oncol 2011;38:113–20.

27) Li Y, Tredget EE, Ghaffari A, Lin X, Kilani RT, Ghahary A. Local expression of indoleamine 2,3-dioxygenase protects engraftment of xenogeneic skin substitute. J Invest Dermatol 2006;126:128–36.

28) Metz R, Duhadaway JB, Kamasani U, Laury-Kleintop L, Muller AJ, Prendergast GC. Novel tryptophan catabolic enzyme IDO2 is the preferred biochemical target of the antitumor indoleamine 2,3-dioxygenase inhibitory compound D-1-methyl-tryptophan. Cancer Res 007;67:7082–7.

29) Sharma MD, Hou DY, Liu Y, Koni PA, Metz R, Chandler P, et al. Indoleamine 2,3-dioxygenase controls conversion of Foxp3Tregs to TH17-like cells in tumor-draining lymph nodes. Blood 2009;113:6102–11.

30) Ostrand-Rosenberg, S., Clements, VK., Terabe, M., Park, JM., Berzofsky, JA., Dissanayake SK. Resistance to metastatic disease in STAT6-deficient mice rquires hemopoietic and nonhemopoietic cells and is IFN-gamma dependent. J. Immunol. 2002; 169: 5796-804

APPENDICIES:

1. Figures 1 to 11.

2. Courtney Smith, Mee Young Chang, Katherine H. Parker, Daniel W. Beury, James B. DuHadaway, Hollie E. Flick, Janette Boulden, Erika Sutanto-Ward, Alejandro Peralta Soler, Lisa D. Laury-Kleintop, Laura Mandik-Nayak, Richard Metz, Suzanne Ostrand-Rosenberg, George C. Prendergast, and Alexander J. Muller. (2012) IDO Is a Nodal Pathogenic Driver of Lung Cancer and Metastasis Development. *Cancer Discov; 2(8); 1–14.*

3. Supplementary Figures 1 to 3.

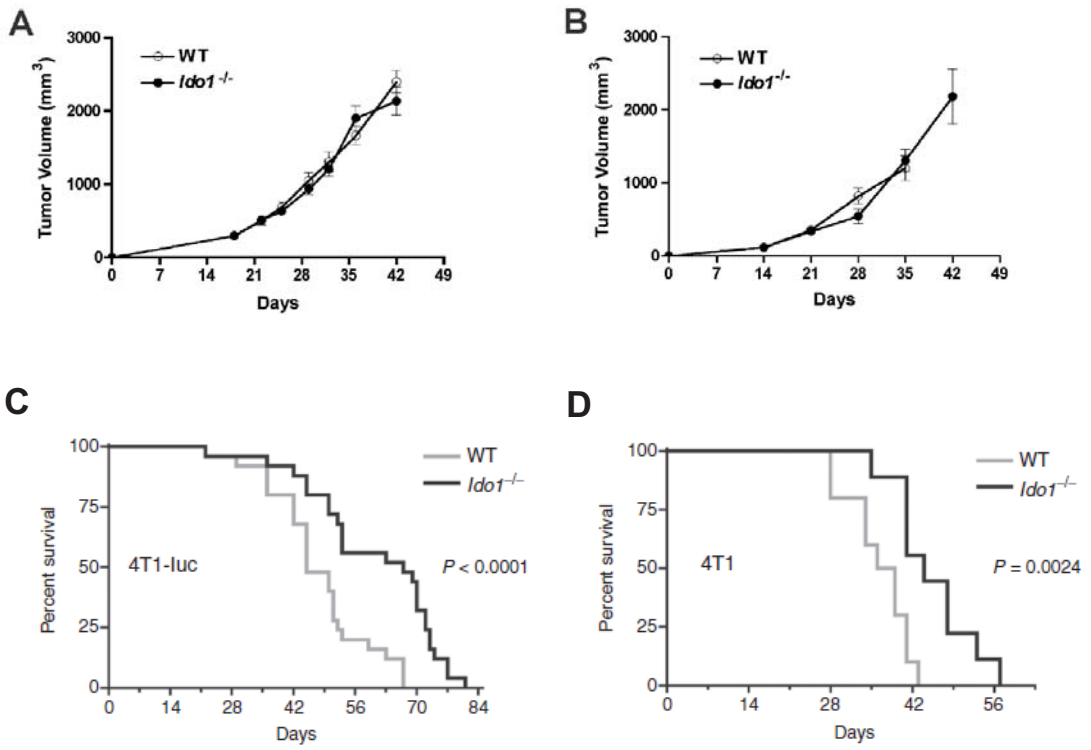

Figure 1: IDO deficiency delays the development of pulmonary metastases but not primary tumor growth. (A,B) Primary 4T1 tumor growth is unaffected in *Ido1-/-* mice. WT and *Ido1-/-* mice received orthotopic grafts of (A) 4T1-luc (N = 20) or (B) 4T1 (N = 5) cells. Beginning at approximately 14 days, when a palpable tumor mass had become apparent, caliper measurements were made on a weekly basis to calculate primary tumor volumes. The data are plotted as means ± SE. Measurements for WT mice challenged with 4T1 cells at 42 days were not collected due to metastasis-associated mortality in this group. (C,D) Kaplan-Meier survival curves for cohorts of WT and *Ido1-/-* mice following orthotopic engraftment of 1 x 10^4 (C) 4T1-luc (n = 25) or (D) 4T1 (n ≥ 9) tumor cells. Significance was assessed by 2-group log-rank test at $P < 0.05$. The survival benefit observed in *Ido1-/-* mice was independently replicated at University of Maryland Baltimore County.

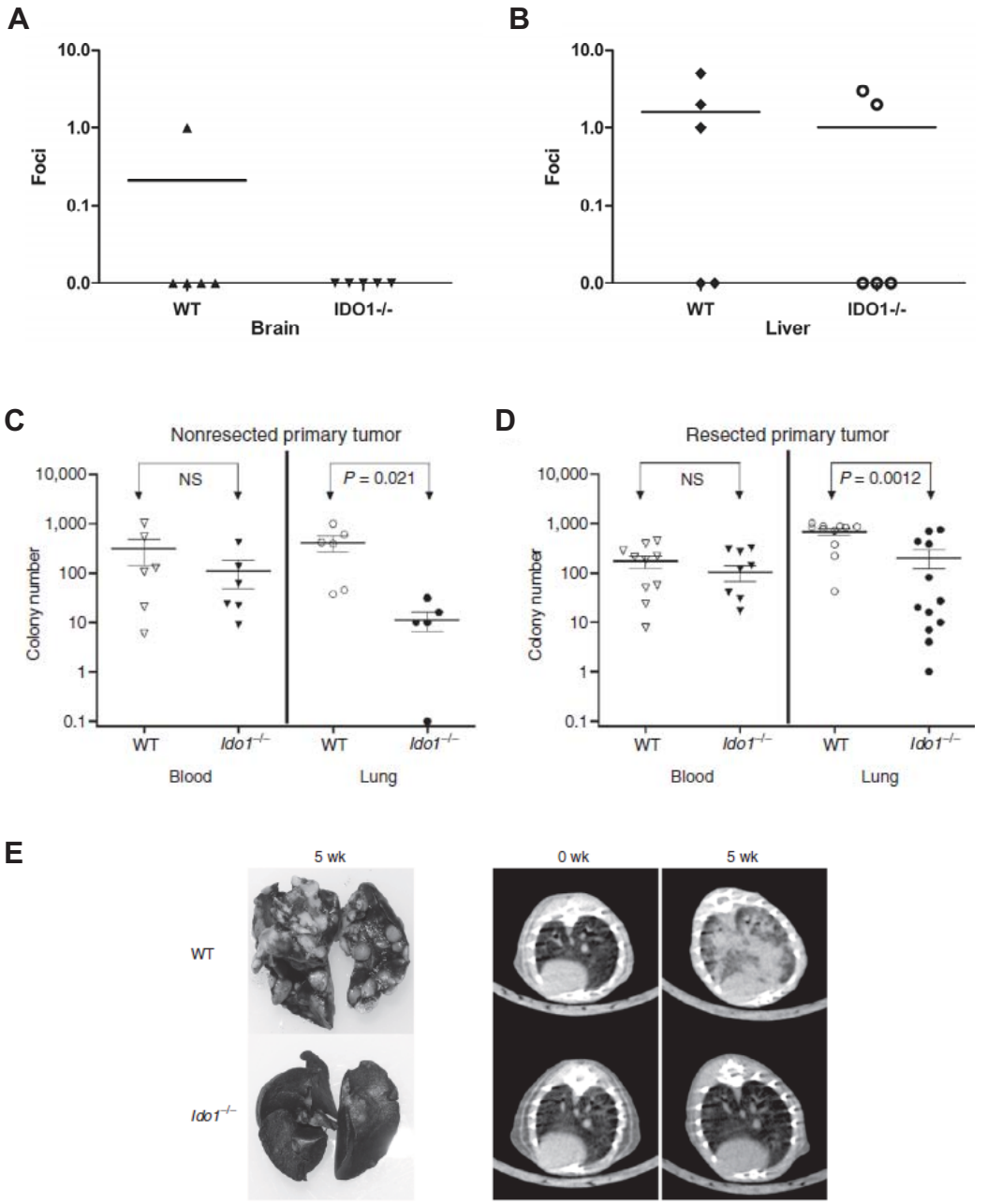

Figure 2: *Ido1-/-* mice show reduced pulmonary metastases compared to WT mice. (A-B) *Ido1-/-* mice exhibit no demonstrable resistance to 4T1 brain (A) or liver (B) metastasis formation. At 6 weeks following orthotopic injection of 4T1-luc cells into WT and *Ido1-/-* hosts (N = 5 per group), colony forming assays were performed to assess the relative tumor cell burden in the liver. Individual data points are graphed as a scatter plot on a log scale together with the means ± SE. Because the data are plotted on a log scale, points with a value of 0 are not represented in the scatter plot but were included in computing the means. (C-D) At 5 weeks following (C) orthotopic engraftment of 4T1 cells (n = 6) or (D) orthotopic engraftment of 4T1 cells and resection of the primary tumor at 18 days postengraftment (n ≥ 11), colony forming assays were conducted to assess the relative tumor cell burden in the blood (neat) and lungs (1:1000). Individual data points are graphed on a log scale scatter plot with the means ± SEM and significance assessed by 2-tailed Student t test at $P < 0.05$ (NS, not significant). (E) Staining of lung with India Ink and axial images from micro-CT scans depicting the difference in pulmonary metastasis burden between WT and *Ido1-/-* mice at 5 weeks following orthotopic 4T1 tumor cell engraftment.

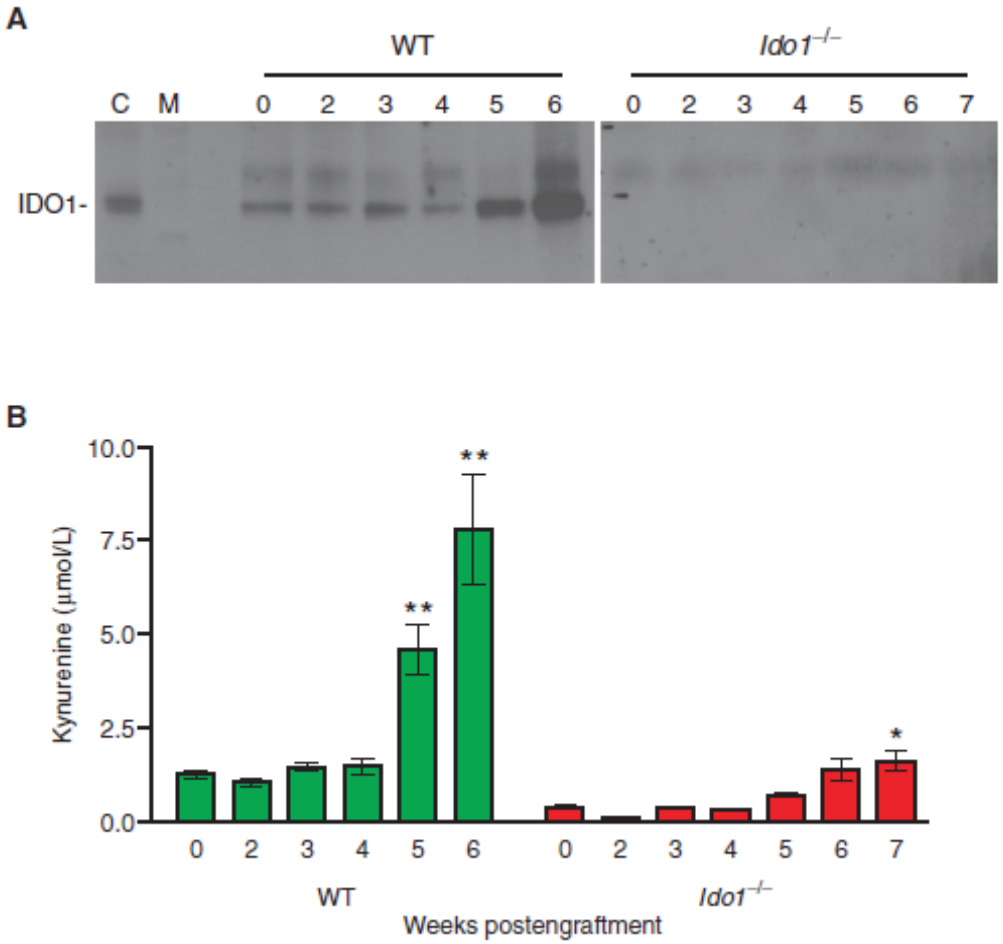

Figure 3: IDO protein and activity correlates with increased 4T1 tumor metastasis. (A) Evaluation of IDO1 protein levels by immunoprecipitation-Western blot analysis of lung tissue lysates from WT and *Ido1-/-* mice following orthotopic engraftment of 4T1 tumor cells at the time points in weeks indicated above each lane. C. epididymis lysate positive control lane; M, molecular weight marker lane. (B) Evaluation of kynurenine levels by LC/MS-MS-based analysis of homogenized lung samples from WT and *Ido1-/-* mice following orthotopic engraftment of 4T1 tumor cells at the time points in weeks indicated for each lane. Means ± SEM ($n \geq 6$) are graphed with significance relative to baseline determined by one-way ANOVA with Dunn test (*, $P<0.05$; **, $P<0.01$).

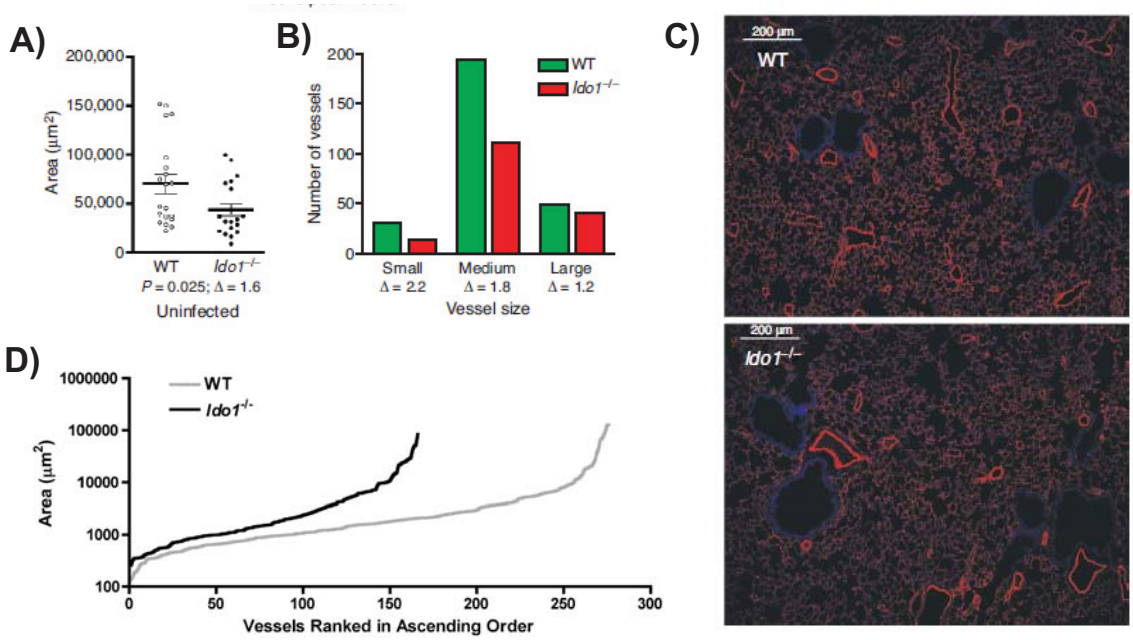

Figure 4: Vascular density is reduced in the lungs of *Ido1-/-* mice. (A) Volumetric image analysis of tumor and vasculature performed on the 3-D reconstructions of lung micro-CT images. The data are graphed as a scatter plot with the means ± SEM (Δ; fold difference). Significance was determined by two-tailed Student's *t* test at $P < 0.05$. (B) Distribution of pulmonary vessels within specified size ranges. The total number of small (<500 µm^2), medium (500-5000 µm^2) and large (>5000 µm^2) vessels identified within the defined fields evaluated in D are plotted on a bar graph (Δ; fold difference. (C) Immunofluorescent staining of blood vessels with antibody to caveolin 1 (red) and DAPI staining of nuclei (blue) in representative lung tissue specimens from WT and *Ido1-/-* mice. Lung tissue sections from 5 WT and 5 *Ido1-/-* mice were stained with anti-caveolin-1 antibody to visualize blood vessels by immunofluorescence. Four images per tissue section were acquired and area measurements of every blood vessel within each field were recorded using AxioVision Release 4.6 software. (D) All of the area measurements were tallied and plotted sequentially in ascending order from smallest to largest with vessel areas graphed on a log scale. The differential in vessel density apparent from this graph is due almost entirely to a reduced number of medium to small sized vessels in the lungs of *Ido1-/-* mice while the number of large vessels (>5,000 µm2) is nearly the same as in the WT mice.

A)

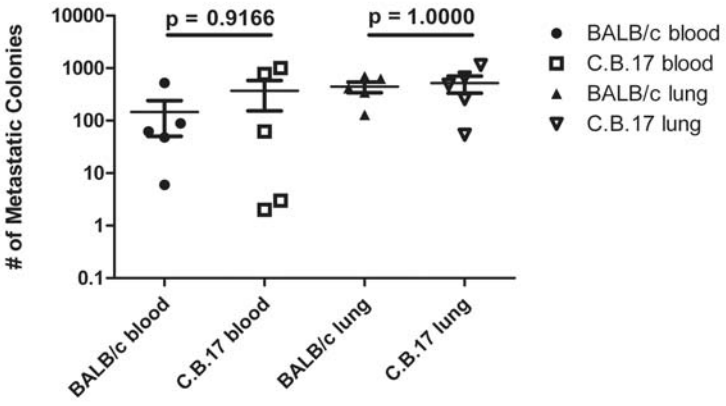

B)

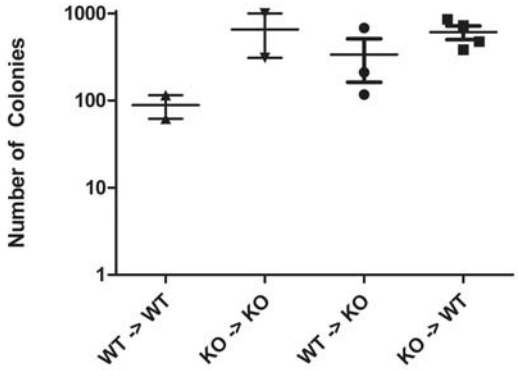

C)

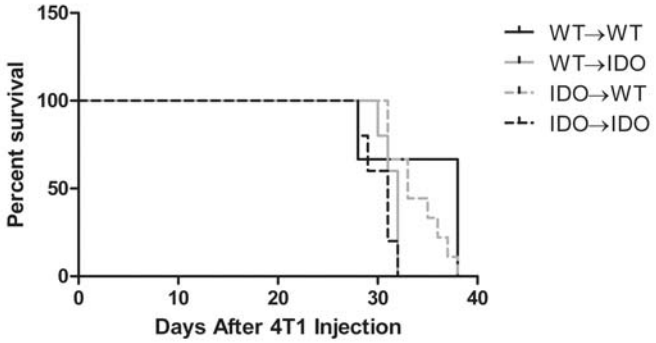

Figure 5: Bone Marrow Chimera Experiments**.** (A) Lung tissue was homogenized and blood collected 6 weeks following orthotopic engraftment of 4T1 cells into BALB/c and C.B-17 mice. Colony forming assay to measure metastatic spread showed equal metastatic burden in BALB/c mice and C.B-17 mice. (B) Following bone marrow transplant, colony forming assay shows that control experiments run the opposite of expected, with *Ido1-/-* to *Ido1-/-* mice having greater metastatic burden compared to WT to WT mice. (C) A small cohort in a survival assay had similar results with WT to WT mice surviving longer than *Ido1-/-* to *Ido1-/-* mice, negating the use of either experiment.

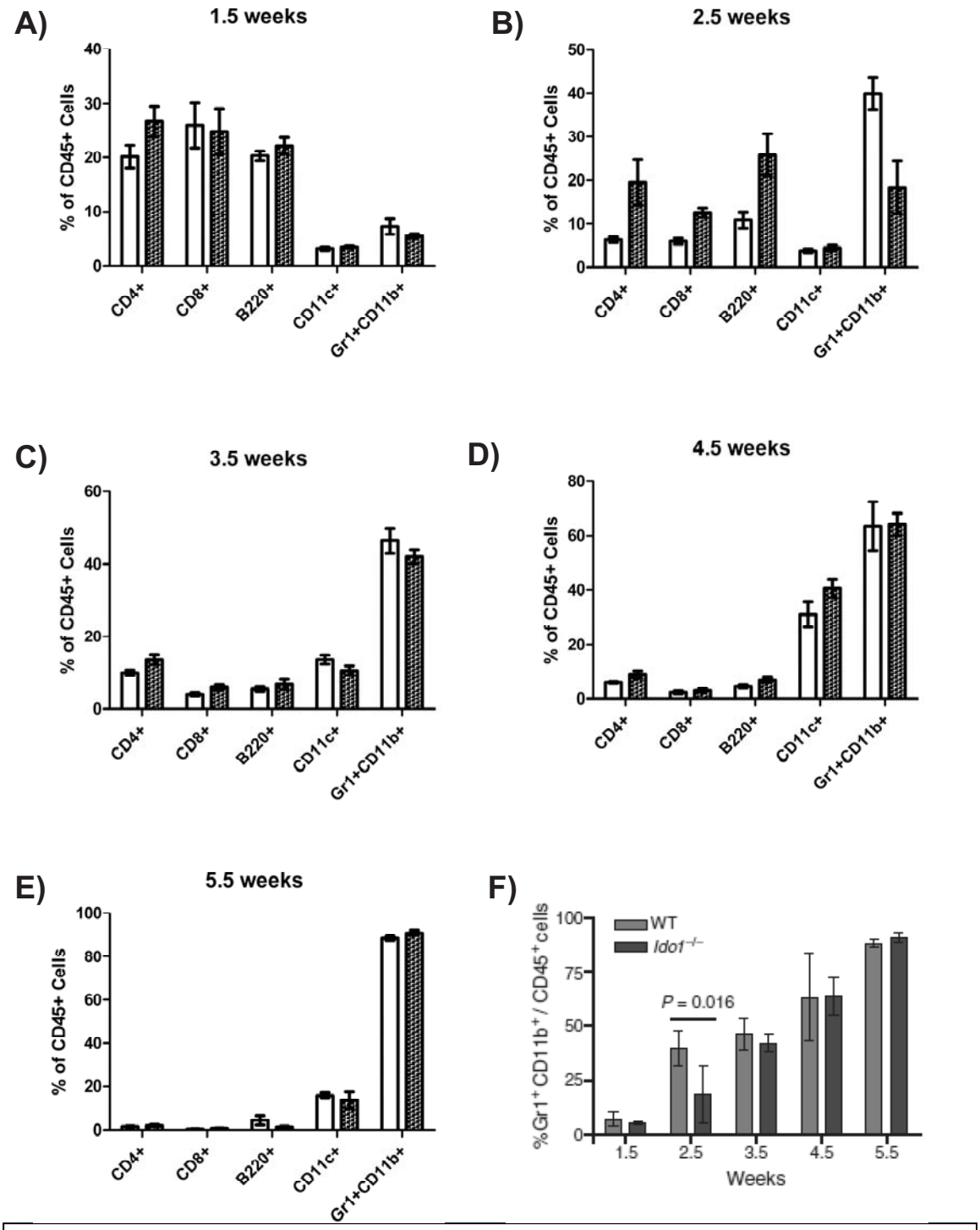

Figure 6: MDSCs are elevated early in WT mice. Whole lung tissues from WT and *Ido1-/-* mice at weekly time intervals were enzymatically digested to single cell suspensions for analysis by flow cytometry. Immune cells were selected by gating on CD45+ cells. Cells were further identified for T-cells (CD4+ and CD8+), B-cells (B220+), macrophages (CD11c+) and the MDSC cell type by Gr1+CD11b+ expression. Immune cell profiles were measured at (A) 1.5 weeks, (B) 2.5 weeks, (C) 3.5 weeks, (D) 4.5 weeks and (E) 5.5 weeks following orthotopic injection. (F) Comparison of MDSCs over time course.

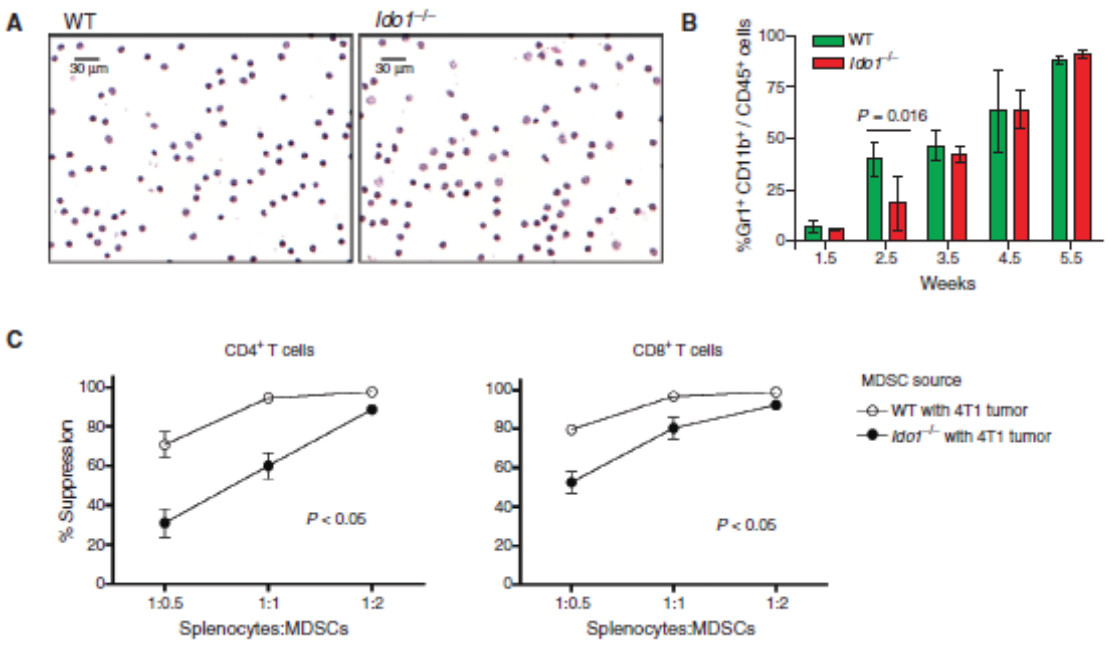

Figure 7: MDSCs from *Ido1-/-* mice are less suppressive. (A) Comparative microscopic images of H&E-stained MDSCs harvested from the blood of WT and *Ido1*$^{-/-}$ mice with primary 4T1 tumors that were not significantly different in size (12.2 ± 1.36 and 11. 5± 0.4 mm in diameter, respectively). (**B**) Single cell suspensions of whole lung tissues were prepared at the indicated time points following 4T1 engraftment into WT and *Ido1*$^{-/-}$ mice and evaluated by flow cytometry for MDSC infiltration by gating on CD45^{+} cells and analyzing the Gr1^{+} CD11b^{+} cell population. Means ± SEM are graphed with significance assessed by two-tailed Student's *t* test at $P < 0.05$. (C) Splenocytes from CD4^{+} TS1 (*left*) or CD8^{+} Clone 4 (*right*) mice were co-cultured in triplicate with cognate peptide and increasing proportions of 4T1-induced, peripheral blood MDSCs from WT or *Ido1*$^{-/-}$ mice. T cell activation was quantified by uptake of ^{3}H-thymidine and graphed as percent suppression relative to activation in the absence of MDSCs. Significance was assessed by Wilcoxon Rank test at $P < 0.05$. Outcomes are representative of a minimum of 3 independent experiments.

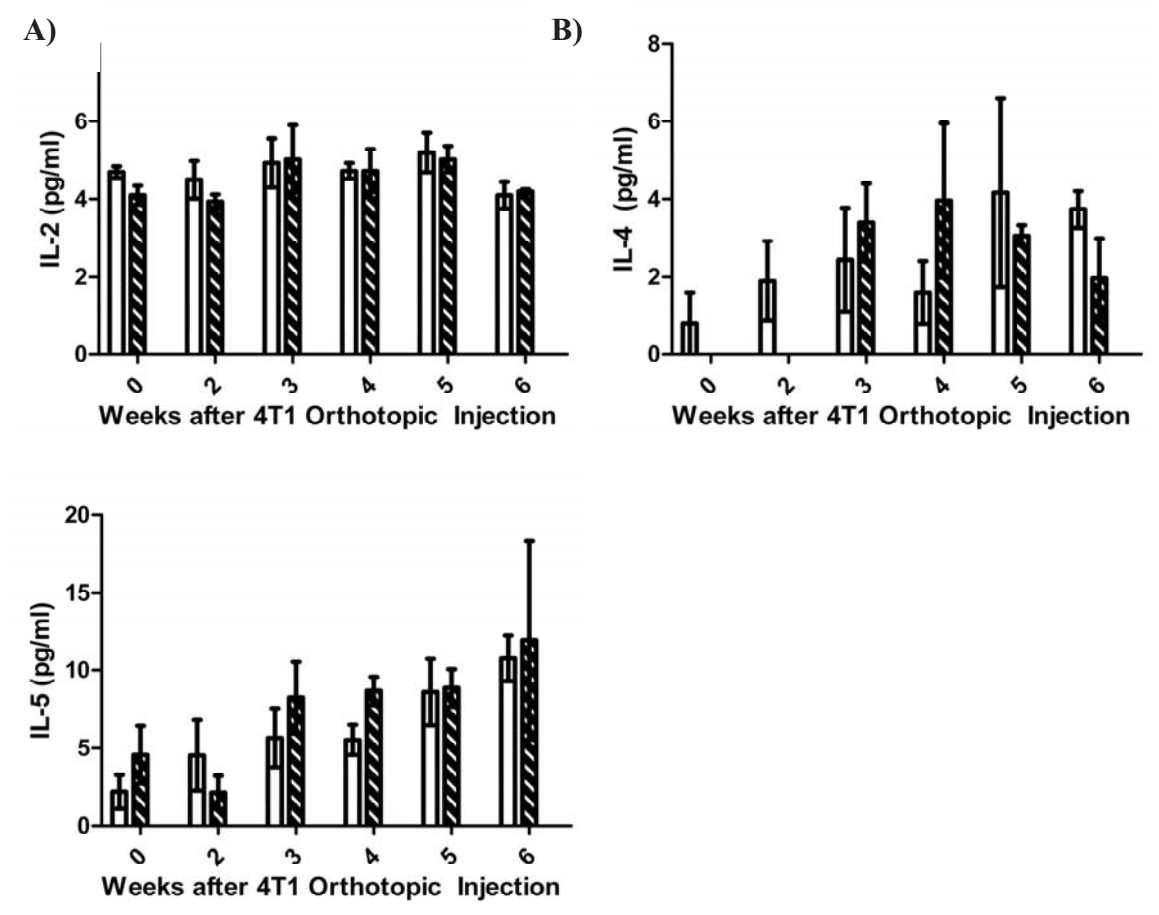

Figure 8: Metastasis does not affect Th1/Th2/Th17 cytokines. Homogenized lung tissue was analyzed for a panel of cytokines using the cytokine bead array. Cytokines are graphed as the average cytokine level in lung of five mice as a factor of time. Data shows mean and SEM. Neither IL-2, IL-4 nor IL-5 showed significant induction in either WT and IDO1-/- mice.

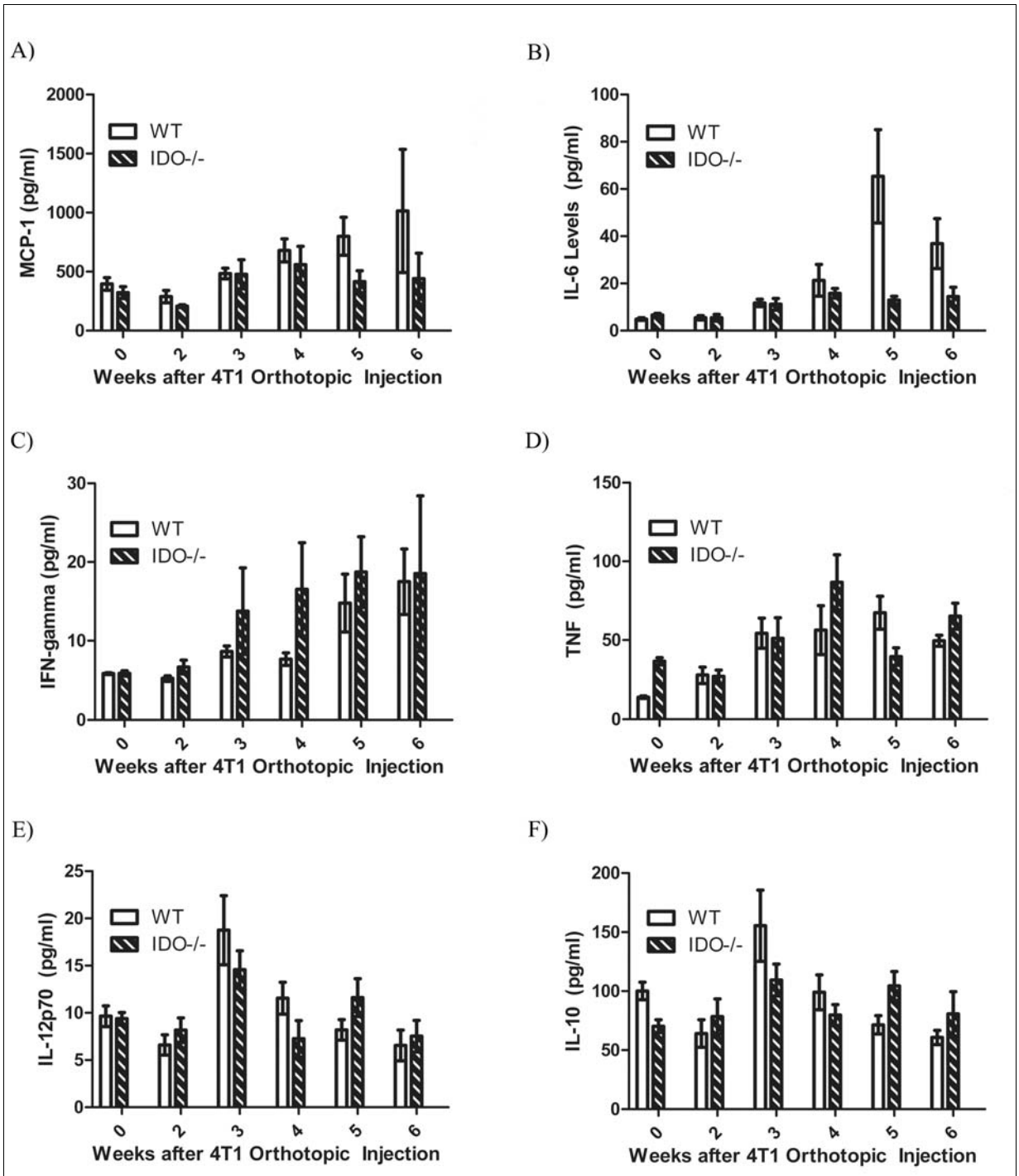

Figure 9 Metastasis induces inflammatory cytokines. Homogenized lung tissue was analyzed for a panel of cytokines using the cytokine bead array. Cytokines are graphed as the average cytokine level in lung of five mice as a factor of time. Data shows mean and SEM. (A) MCP-1 levels are induced as early as 3 weeks and continue to elevate beyond that of *Ido1*-/- mice. (B) IL-6 levels similarly increase and are maximally induced at 6 weeks. (C-D) IFN-γ and TNF levels are induced maximally at 5 weeks in both WT and *Ido1*-/- mice. (E-F) Neither IL-12p70 nor IL-10 showed significant changes in induction between WT and *Ido1*-/- mice.

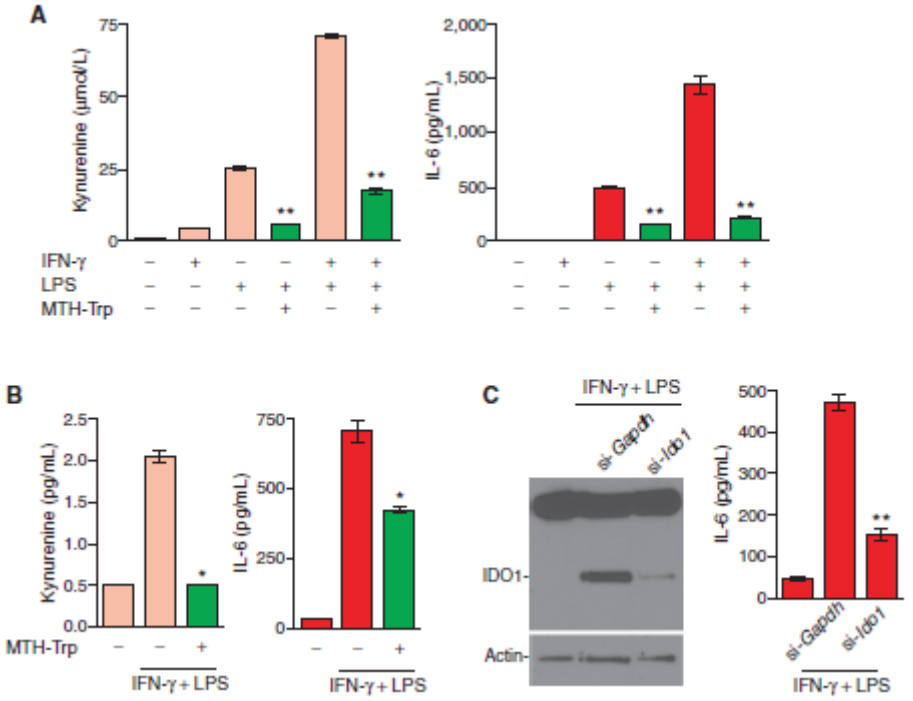

Figure 10: IDO-dependent potentiation of IL6 production. (A) Supernatant from U937 cells stimulated for 24 hours with IFNγ (100 ng/ml) and/or LPS (100 ng/ml) was analyzed for kynurenine and IL6. Results from triplicate plates are plotted as the means ± SEM. Methyl thiohydantoin tryptophan (MTH-Trp, 100 μmol/l) was included during induction where indicated and significance relative to the corresponding induced level without MTH-Trp was determined by two-tailed Student's *t* test (**; $P \leq 0.0001$). (B) Supernatant from HL-60 cells stimulated for 24 hours with IFNγ (100 ng/ml) and LPS (100 ng/ml) was analyzed for kynurenine and IL6. Results from duplicate plates are plotted as the means ± SEM. Methyl thiohydantoin tryptophan (MTH-Trp, 100 μmol/l) was included during induction where indicated and significance relative to the corresponding induced level without MTH-Trp was determined by two-tailed Student's *t* test (*; $P < 0.05$). (C) HL-60 cells treated in triplicate with *Ido1*-targeting (si-*Ido1*) or non-targeting (si-*Gapdh*) siRNAs were stimulated for 24 hours with IFNγ (100 ng/ml) and LPS (100 ng/ml). Pooled cell lysates were analyzed by Western blot analysis for IDO1 and actin (*left panel*) and individual cell supernatants were analyzed for IL6 (*right panel*). The IL6 data are plotted as the means ± SEM with the significance of the difference between specific *Ido1*-targeting versus non-targeting results determined by two-tailed Student's *t* test (**; $P < 0.0001$).

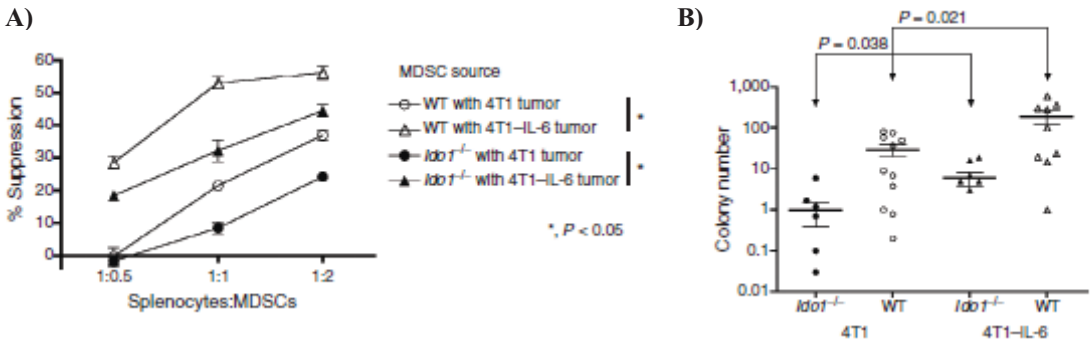

Figure 11: Attenuated MDSC suppressive activity and metastasis development in IDO-deficient mice is rescued by IL6. (A) Splenocytes from $CD8^+$ Clone 4 transgenic mice were co-cultured with cognate peptide and increasing proportions of 4T1 or 4T1-IL6 tumor-induced MDSCs from WT or *Ido1*$^{-/-}$ mice for analysis as in B. Outcomes are representative of 6 independent experiments using TS1, Clone 4, or DO11.10 transgenic T cells. (B) Colony forming assays to assess the relative tumor cell burden in the lungs performed 6 weeks following intravenous injection of 4T1 or 4T1-IL6 cells into WT and *Ido1*$^{-/-}$ mice. Results are presented on log scale scatter plot with means ± SEM. Significance was assessed by two-tailed Student's *t* test at $P < 0.05$.

CANCER DISCOVERY

IDO Is a Nodal Pathogenic Driver of Lung Cancer and Metastasis Development

Courtney Smith, Mee Young Chang, Katherine H. Parker, et al.

Cancer Discovery Published OnlineFirst July 19, 2012.

Published OnlineFirst on July 19, 2012; DOI:10.1158/2159-8290.CD-12-0014

RESEARCH ARTICLE

IDO Is a Nodal Pathogenic Driver of Lung Cancer and Metastasis Development

Courtney Smith[1], Mee Young Chang[1], Katherine H. Parker[3], Daniel W. Beury[3], James B. DuHadaway[1], Hollie E. Flick[1,4], Janette Boulden[1], Erika Sutanto-Ward[1], Alejandro Peralta Soler[1,7], Lisa D. Laury-Kleintop[1], Laura Mandik-Nayak[1], Richard Metz[2], Suzanne Ostrand-Rosenberg[3], George C. Prendergast[1,5,6], and Alexander J. Muller[1,6]

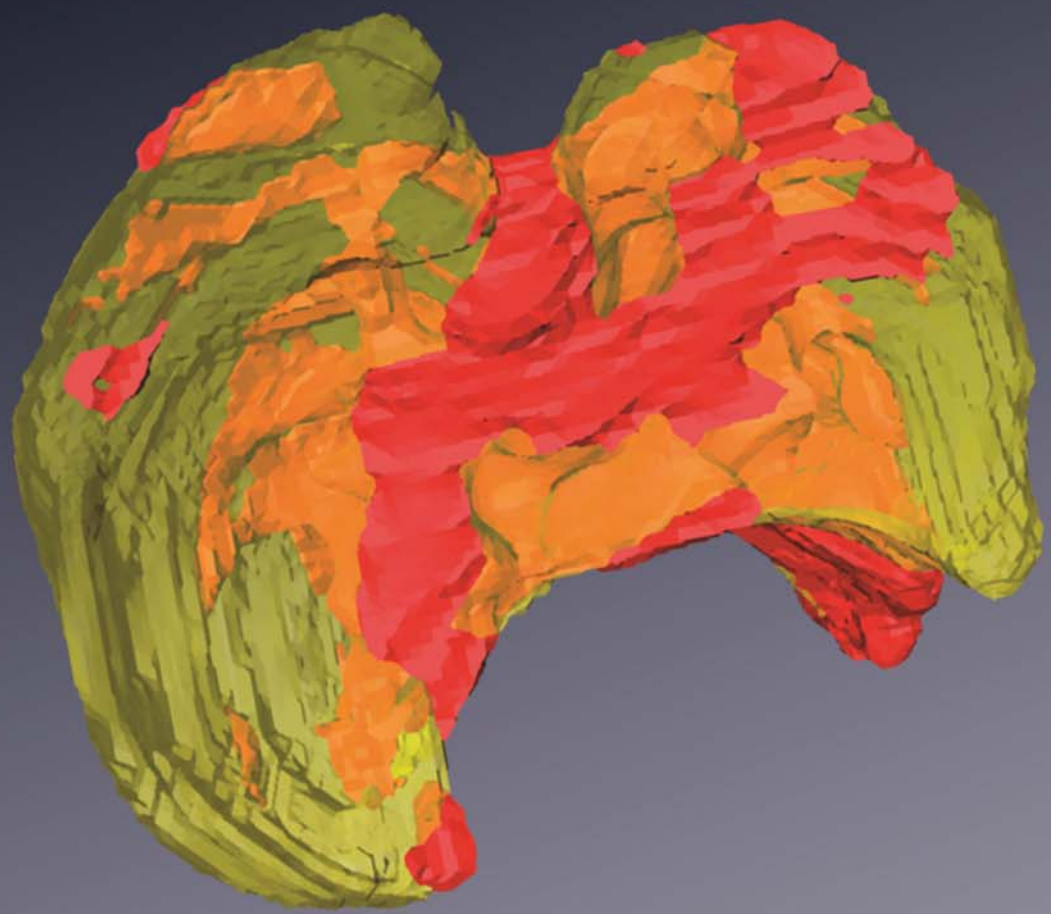

Published OnlineFirst on July 19, 2012; DOI:10.1158/2159-8290.CD-12-0014

ABSTRACT

Indoleamine 2,3-dioxygenase (IDO) enzyme inhibitors have entered clinical trials for cancer treatment based on preclinical studies, indicating that they can defeat immune escape and broadly enhance other therapeutic modalities. However, clear genetic evidence of the impact of IDO on tumorigenesis in physiologic models of primary or metastatic disease is lacking. Investigating the impact of *Ido1* gene disruption in mouse models of oncogenic KRAS-induced lung carcinoma and breast carcinoma–derived pulmonary metastasis, we have found that IDO deficiency resulted in reduced lung tumor burden and improved survival in both models. Micro-computed tomographic (CT) imaging further revealed that the density of the underlying pulmonary blood vessels was significantly reduced in *Ido1*-nullizygous mice. During lung tumor and metastasis outgrowth, interleukin (IL)-6 induction was greatly attenuated in conjunction with the loss of IDO. Biologically, this resulted in a consequential impairment of protumorigenic myeloid-derived suppressor cells (MDSC), as restoration of IL-6 recovered both MDSC suppressor function and metastasis susceptibility in *Ido1*-nullizygous mice. Together, our findings define IDO as a prototypical integrative modifier that bridges inflammation, vascularization, and immune escape to license primary and metastatic tumor outgrowth.

SIGNIFICANCE: This study provides preclinical, genetic proof-of-concept that the immunoregulatory enzyme IDO contributes to autochthonous carcinoma progression and to the creation of a metastatic niche. IDO deficiency *in vivo* negatively impacted both vascularization and IL-6–dependent, MDSC-driven immune escape, establishing IDO as an overarching factor directing the establishment of a protumorigenic environment. *Cancer Discov; 2(8); 1–14. ©2012 AACR.*

INTRODUCTION

Inflammatory tissue microenvironments contribute strongly to tumor progression, but due to the complex multifactorial nature of inflammation, there remains limited understanding of specific pathogenic components that might be targeted to effectively treat cancer (1). In this context, the tryptophan-catabolizing enzyme indoleamine 2,3-dioxygenase (IDO) has emerged as an intriguing target implicated in tumoral immune escape (2, 3). IDO-inhibitory compounds have entered clinical trials based on evidence of immune-based antitumor responses in a variety of preclinical models of cancer (4–10). Meanwhile, inadvertent IDO targeting may already be providing benefits to patients as illustrated by recent evidence that the clinically approved tyrosine kinase inhibitor imatinib dampens IDO induction as a key mechanism for achieving therapeutic efficacy in the treatment of gastrointestinal stromal tumors (11).

Authors' Affiliations: [1]Lankenau Institute for Medical Research; [2]NewLink Genetics Corporation, Wynnewood, Pennsylvania; [3]Department of Biological Sciences, University of Maryland Baltimore County, Baltimore, Maryland; [4]Department of Biochemistry, Drexel University College of Medicine; [5]Department of Pathology, Anatomy, and Cell Biology, [6]Kimmel Cancer Center, Thomas Jefferson University, Philadelphia, Pennsylvania; and [7]Richfield Laboratory of Dermatopathology, Cincinnati, Ohio

Note: Supplementary data for this article are available at Cancer Discovery Online (http://cancerdiscovery.aacrjournals.org/).

C. Smith and M.Y. Chang contributed equally to this study.

Corresponding Authors: Alexander J. Muller and George C. Prendergast, Lankenau Institute for Medical Research, 100 Lancaster Avenue, Wynnewood, PA 19096. Phone: 484-476-8034 or 8475; Fax: 484-476-8533; E-mail: mullera@mlhs.org or prendergast@limr.org

doi: 10.1158/2159-8290.CD-12-0014

Although results with IDO pathway inhibitors are provocative, the conclusions that can be drawn are inherently limited by drug specificity concerns, especially in the absence of independent genetic validation. Addressing this issue, our studies on the impact of *Ido1* gene deletion on 7,12-dimethylbenz(*a*)anthracene/12-*O*-tetradecanoylphorbol-l3-acetate (DMBA/TPA)-elicited skin papillomagenesis established that IDO has an integral tumor-promoting role in the context of phorbol ester–elicited inflammation (12, 13), but interpretation of these results is tempered by the possibility that the chemical exposures in this model may produce anomalies irrelevant to the majority of spontaneous tumors. The lungs present a particularly compelling physiologic context in which to further investigate the role of IDO in tumorigenesis as IDO is known to be highly inducible in this tissue (14, 15), and there is an urgent unmet medical need for effective therapeutic options to treat primary lung tumors and metastases. In this report, we investigated the consequences of IDO loss through genetic ablation in the context of well-established, pulmonary models of oncogenic KRAS-induced adenocarcinoma and orthotopic breast carcinoma metastasis. Our findings reveal previously unappreciated roles for IDO in vascularization and in the production of the proinflammatory cytokine interleukin (IL)-6 that in turn dictates the development of protumorigenic, myeloid-derived suppressor cells (MDSC).

RESULTS

IDO Deficiency Prolongs the Survival of Mice with Sporadic *Kras*^{G12D}-Driven Lung Carcinomas

LSL-Kras^{G12D} (*Lox-Stop-Lox Kras*^{G12D}) transgenic mice develop sporadic focal pulmonary adenocarcinomas following intranasal administration of *Cre*-expressing adenovirus vector

Published OnlineFirst on July 19, 2012; DOI:10.1158/2159-8290.CD-12-0014

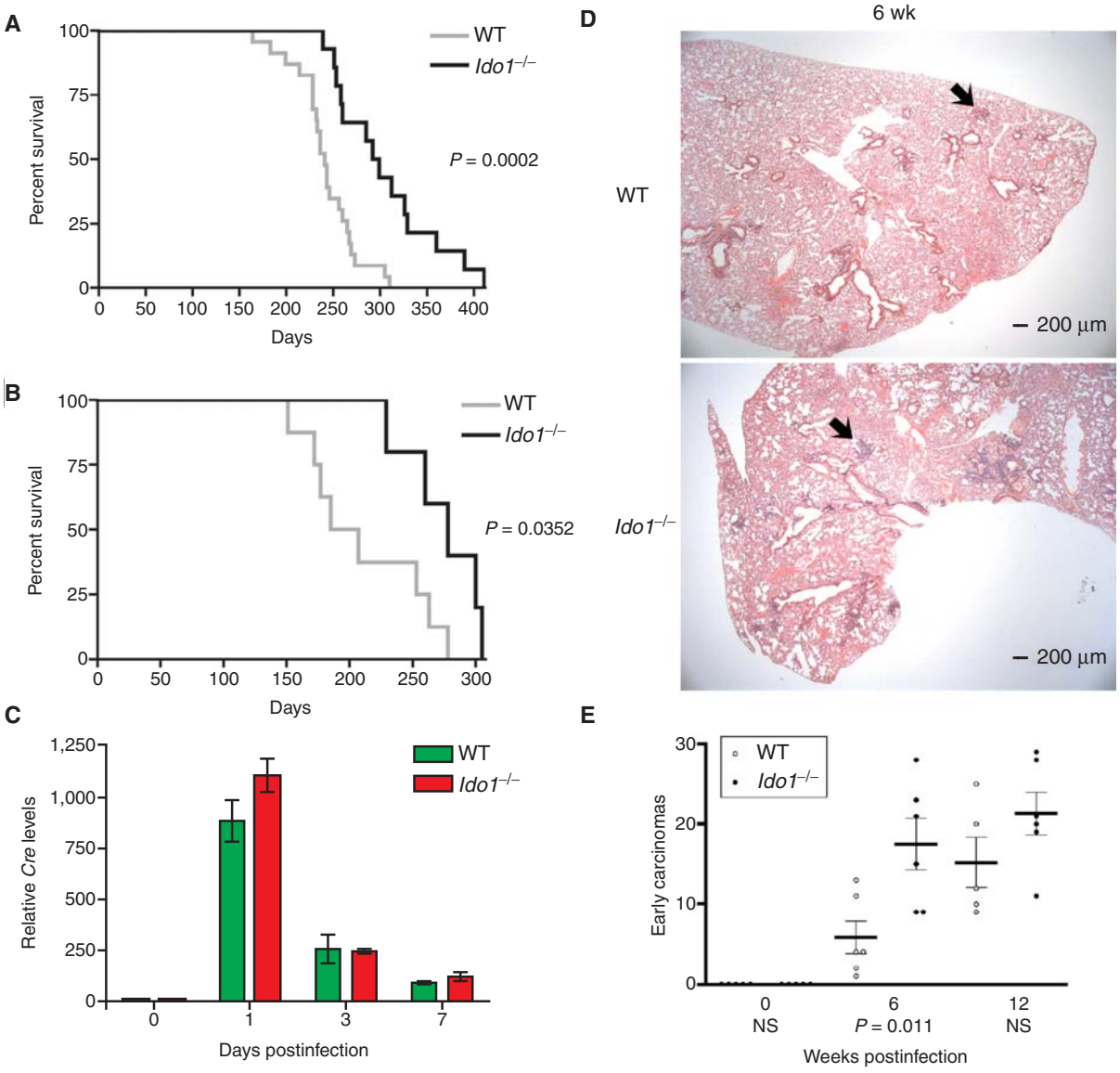

Figure 1. IDO deficiency extends the survival of mice with KRAS-induced lung adenocarcinomas despite an elevated number of early lesions. **A,** Kaplan–Meier survival curves for cohorts of *Lox-Kras*^{G12D} ($n = 23$) and *Ido1*$^{-/-}$ *Lox-Kras*^{G12D} ($n = 14$) mice infected with 2.5×10^7 plaque-forming units (pfu) of Ad-*Cre* virus. **B,** Kaplan–Meier survival curves for cohorts of *Lox-Kras*^{G12D} ($n = 8$) and *Ido1*$^{-/-}$ *Lox-Kras*^{G12D} ($n = 5$) mice infected with 1.25×10^8 pfu Ad-*Cre* virus. Significance for both data sets was assessed by 2-group log-rank test at $P < 0.05$. **C,** total lung DNA prepared from 3 mice per time point was analyzed for the presence of the viral *Cre* gene by real-time PCR at 0, 1, 3, and 7 days postinfection. Relative *Cre* levels determined from this analysis are plotted as means ± SEM. **D,** representative hematoxylin and eosin (H&E)-stained sections depicting the observed difference in early lesions between the lungs of *Lox-Kras*^{G12D} and *Ido1*$^{-/-}$ *Lox-Kras*^{G12D} mice at 6 weeks postinfection. **E,** quantitative histopathologic assessment of lesion frequency in H&E-stained sections of lung biopsies from *Lox-Kras*^{G12D} and *Ido1*$^{-/-}$ *Lox-Kras*^{G12D} mice at 6 and 12-week postinfection ($n \geq 5$). The number of lesions identifiable under low magnification within a defined region of each specimen are graphed on the scatter plot with the means ± SEM. Significance was determined by 2-tailed Student *t* test at $P < 0.05$. NS, not significant.

(Ad-*Cre*) to activate the latent oncogenic *Kras*^{G12D} allele (16). These RAS-induced adenocarcinomas elicit a robust inflammatory response (17) wherein IDO may impart a protumorigenic skew (2). To investigate this hypothesis in an autochthonous lung tumor setting, we introduced *Ido1*$^{-/-}$ (homozygous *Ido1*-null) alleles (18) into the *LSL-Kras*^{G12D} mouse strain. *Ido1*$^{-/-}$ *Lox-Kras*^{G12D} mice displayed significantly increased survival relative to *Lox-Kras*^{G12D} mice at 2 different multiplicities of Ad-*Cre* infection (Fig. 1A and B). Similar levels of *Cre* were present in the lungs of both strains at 0, 1, 3, and 7 days postinfection (Fig. 1C). Unexpectedly, histopathologic examination at 6 weeks revealed that the frequency of early precancerous lesions was actually about 3-fold higher in the *Ido1*$^{-/-}$ *Lox-Kras*^{G12D} mice (Fig. 1D and E), substantiating

Published OnlineFirst on July 19, 2012; DOI:10.1158/2159-8290.CD-12-0014

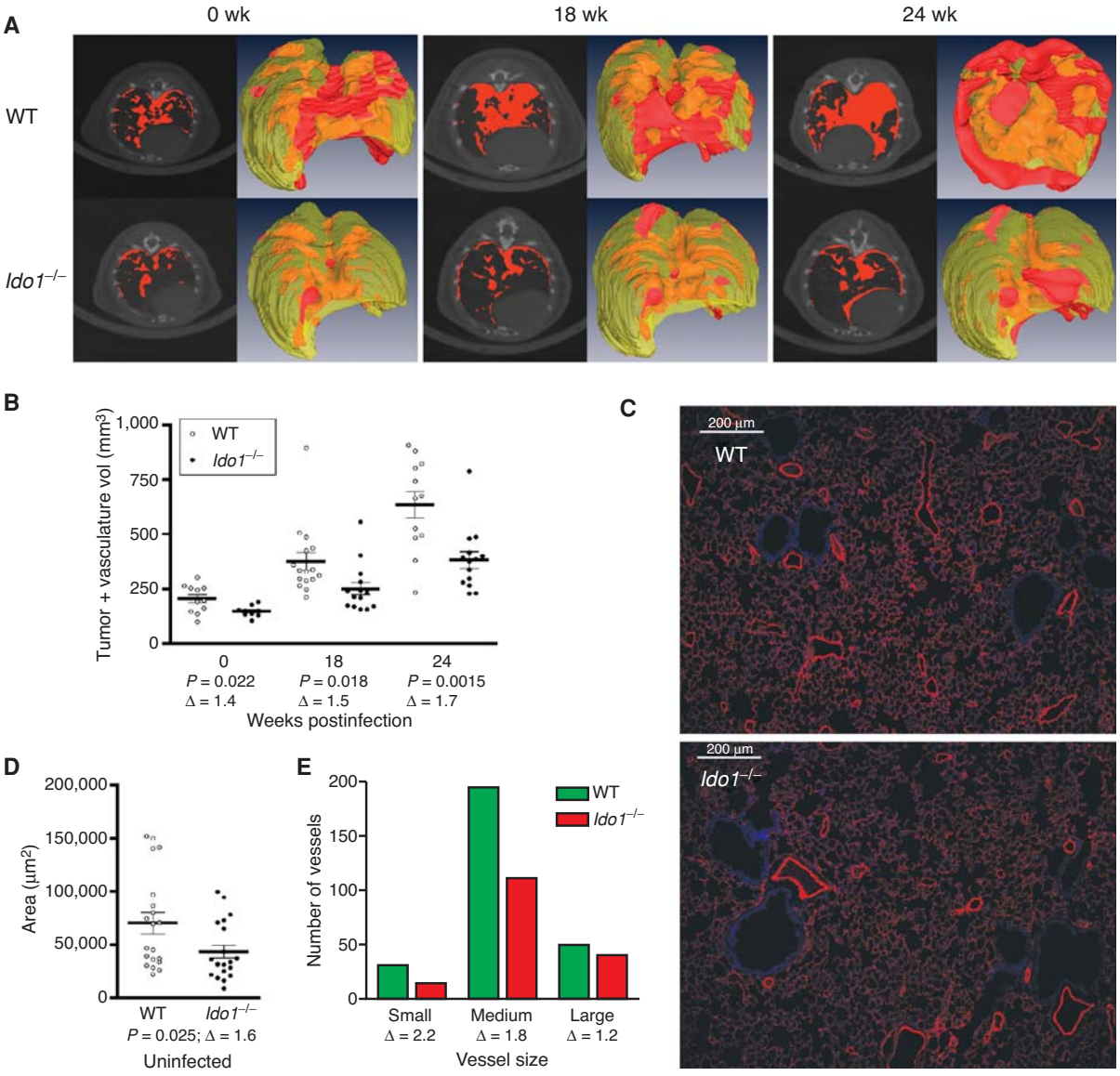

Figure 2. IDO deficiency impairs the outgrowth of overt lung adenocarcinomas and reduces normal pulmonary vascularization. **A,** representative axial micro-CT images and 3D reconstructions of *Lox-Kras*^{G12D} and *Ido1*$^{-/-}$ *Lox-Kras*^{G12D} mouse lungs acquired at 0, 18, and 24 weeks postinfection. Tumor and vasculature, which have indistinguishable x-ray densities, are designated in red in the individual CT images (left) or red/orange for exterior/interior location in the 3D reconstructions (right). **B,** volumetric image analysis of tumor and vasculature conducted on the 3D reconstructions of lung micro-CT images. The data are graphed as a scatter plot with the means ± SEM (Δ; fold difference). Significance was determined by 2-tailed Student *t* test at $P < 0.05$. **C,** immunofluorescent staining of blood vessels with antibody to caveolin 1 (red) and 4′,6-diamidino-2-phenylindole (DAPI) staining of nuclei (blue) in representative lung tissue specimens from BALB/c WT and *Ido1*$^{-/-}$ mice. **D,** quantitation of blood vessel areas. The vessel area totals measured within each field are graphed as a scatter plot with the means ± SEM (Δ; fold difference). Significance was determined by 2-tailed Student *t* test at $P < 0.05$. **E,** distribution of pulmonary vessels within specified size ranges. The total number of small (<500 μm^2), medium (500–5,000 μm^2), and large (>5,000 μm^2) vessels identified within the defined fields evaluated in **D** are plotted on a bar graph (Δ; fold difference). Also see Supplementary Fig. S1C for a graph of individual vessel measurements rank ordered across the entire size range.

that IDO deficiency does not interfere at the stage of Ad-*Cre*–mediated oncogenic RAS activation required to initiate these tumors (ref. 16; Supplementary Fig. S1A). While early tumorigenesis may be negatively impacted by IDO-mediated tryptophan catabolism, as previously proposed (19), this phenomenon was transient with the differential no longer significant by 12 weeks (Fig. 1E).

IDO Deficiency Impairs Tumor Outgrowth and Vascular Development in the Lung

To assess the impact of *Ido1* loss on overt lung tumors, non-invasive micro-computed tomographic (CT) scans were conducted on groups of *Lox-Kras*^{G12D} and *Ido1*$^{-/-}$ *Lox-Kras*^{G12D} mice at 18 and 24 weeks following Ad-*Cre* administration (Fig. 2A).

Published OnlineFirst on July 19, 2012; DOI:10.1158/2159-8290.CD-12-0014

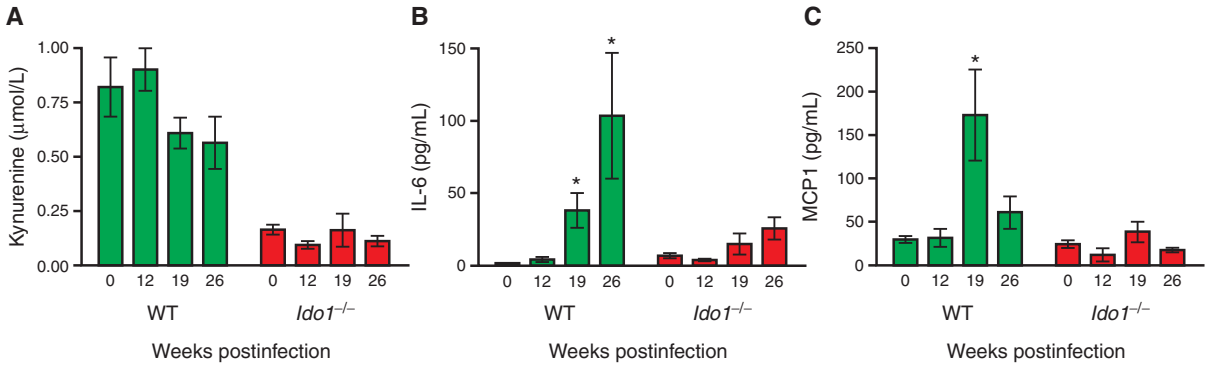

Figure 3. IDO deficiency is associated with attenuated induction of IL-6 and MCP1. **A,** kynurenine levels in the lungs of *Lox-Kras*^{G12D} and *Ido1*$^{-/-}$ *Lox-Kras*^{G12D} mice at 0, 12, 19, and 26 weeks postinfection ($n \geq 3$) assessed by LC/MS-MS analysis and plotted as the means ± SEM. **B** and **C.** IL-6 and MCP1 levels in the lungs of *Lox-Kras*^{G12D} and *Ido1*$^{-/-}$ *Lox-Kras*^{G12D} mice at 0, 12, 19, and 26 weeks postinfection ($n \geq 3$) assessed by multiplexed cytokine bead immunoassay–based analysis and plotted as the means ± SEM with significance relative to baseline determined by one-way ANOVA with Dunn test (*, $P < 0.05$).

Semiautomated quantitative image analysis (20) was conducted on 3-dimensional (3D) reconstructions of the thoracic cavity excluding the heart to assess the combined tumor and vasculature volume within this space. Although lung tumor burden did increase progressively in both cohorts, it was significantly reduced in the *Ido1*$^{-/-}$ *Lox-Kras*^{G12D} mice relative to the corresponding *Ido1*-competent *Lox-Kras*^{G12D} mice (Fig. 2B). Individual micro-CT scan images paired with 3D reconstructions of total chest space and functional lung volume visually highlight the difference in lung tumor burden between representative *Ido1*$^{-/-}$ *Lox-Kras*^{G12D} and *Kras*^{G12D} animals (Fig. 2A; Supplementary Videos). These results indicate that IDO deficiency mitigates overt lung tumor outgrowth, consistent with the increased survival exhibited by these mice.

Micro-CT analysis additionally revealed that the density of normal vasculature in the lungs of uninfected animals was substantially diminished in the *Ido1*$^{-/-}$ animals (Fig. 2A and B). Intriguingly, the difference in vascular density between IDO-deficient and IDO-competent cohorts was proportionately comparable with the difference in overt lung tumor burden at the 18- and 24-week time points (Supplementary Fig. S1B), suggesting an association between the extent of the underlying basal vasculature and the capacity of the lungs to support tumor formation. Immunofluorescent staining of blood vessels in the lungs confirmed the decrease in pulmonary vascular density in *Ido1*$^{-/-}$ animals (Fig. 2C). The area within the lungs occupied by vessels was reduced by about 1.6-fold in *Ido1*$^{-/-}$ animals (Fig. 2D), in line with the differential identified by micro-CT data analysis. Further analysis revealed that the reduction in vascular density occurred predominantly at the level of small- to medium-sized vessels, which were nearly twice as abundant in the wild-type (WT) animals, whereas there was little difference in the number of large vessels (Fig. 2E; Supplementary Fig. S1C).

IDO Promotes IL-6 Elevation during Lung Tumor Formation

In the lungs, IDO is highly responsive to pathogen or cytokine exposure (14, 15). To determine whether lung tumorigenesis also stimulates IDO, we compared steady-state levels of the tryptophan catabolite kynurenine at various times after *Kras*^{G12D} activation. Although baseline levels of kynurenine in the lungs of uninfected *Lox-Kras*^{G12D} mice were significantly higher than in their IDO-deficient counterparts (Fig. 3A), these levels remained constant during lung tumorigenesis (Fig. 3A). In contrast, a multiplexed analysis of inflammatory cytokines at 19 and 26 weeks revealed IL-6 to be elevated by about 25- and 68-fold, respectively, in lungs from tumor-bearing *Lox-Kras*^{G12D} mice but only by about 1- and 3-fold in *Ido1*$^{-/-}$ *Lox-Kras*^{G12D} mice (Fig. 3B). This finding was notable given the known tumor-promoting role of IL-6 in this model (21). Although not of the same magnitude, induction of CCL2/MCP1 [chemokine (C-C motif) ligand 2] was likewise attenuated in tumor-bearing *Lox-Kras*^{G12D} mice lacking *Ido1* (Fig. 3C). In contrast, *Ido1* loss did not significantly affect the relative levels of IL-10, IFN-γ, TNF-α, or IL-12p70 (data not shown).

IDO Deficiency Impedes the Development of Pulmonary Metastases

Given the evidence that *Ido1*$^{-/-}$ mice are resistant to the outgrowth of primary lung tumors, we asked whether *Ido1*$^{-/-}$ animals might exhibit reduced susceptibility to pulmonary metastasis development as well. This question was investigated by orthotopic engraftment of mice with highly malignant 4T1 breast carcinoma cells, which metastasize efficiently to the lungs. Survival was increased significantly in *Ido1*$^{-/-}$ hosts compared with WT hosts after challenge with either a 4T1-luciferase–expressing subclone or with parental 4T1 cells, despite an overall shift in the curves (Fig. 4A and B). No difference in primary tumor growth rate was observed (Supplementary Fig. S2A and S2B), but metastatic lung nodules at necropsy were unambiguously less pronounced in *Ido1*$^{-/-}$ mice (Fig. 4C). Noninvasive micro-CT imaging also confirmed a marked reduction in metastatic burden in *Ido1*$^{-/-}$ mice (Fig. 4C), which was quantified by an *ex vivo* colony-forming assay (ref. 22; Fig. 4D). The metastasis differential was not attributable to reduced intravasation because the same numbers of tumor cells were present in peripheral blood samples from both strains (Fig. 4D). In contrast to lung,

Published OnlineFirst on July 19, 2012; DOI:10.1158/2159-8290.CD-12-0014

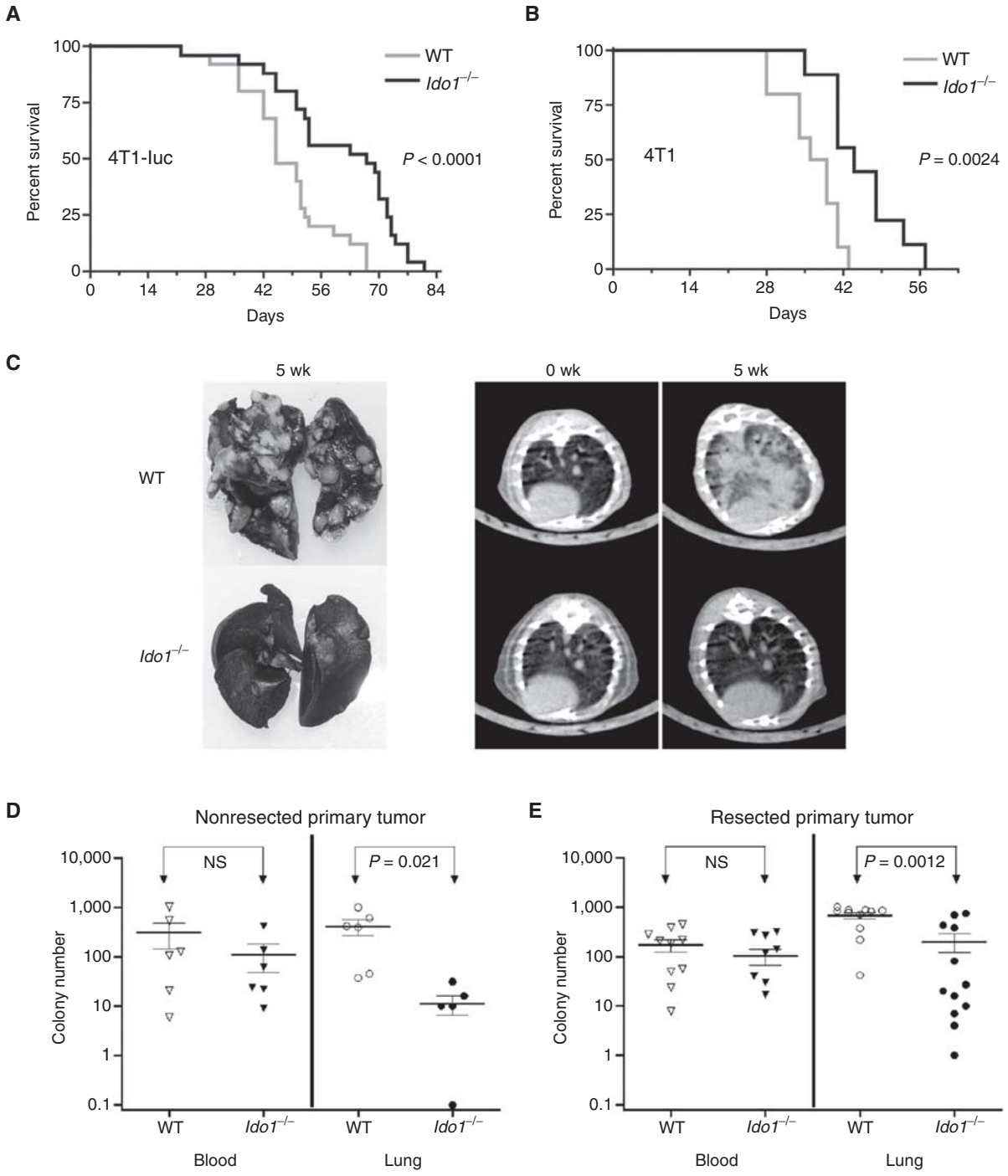

Figure 4. IDO deficiency delays the development of pulmonary metastases. Kaplan–Meier survival curves for cohorts of WT and *Ido1*$^{-/-}$ mice following orthotopic engraftment of 1×10^4 (**A**) 4T1-luc ($n = 25$) or (**B**) 4T1 ($n \geq 9$) tumor cells. Significance was assessed by 2-group log-rank test at $P < 0.05$. The survival benefit observed in *Ido1*$^{-/-}$ mice was independently replicated at University of Maryland Baltimore County. **C,** staining of lungs with India ink and axial images from micro-CT scans depicting the difference in pulmonary metastasis burden between WT and *Ido1*$^{-/-}$ mice at 5 weeks following orthotopic 4T1 tumor cell engraftment. At 5 weeks following (**D**) orthotopic engraftment of 4T1 cells ($n = 6$) or (**E**) orthotopic engraftment of 4T1 cells and resection of the primary tumor at 18 days postengraftment ($n \geq 11$), colony-forming assays were conducted to assess the relative tumor cell burden in the blood (neat) and lungs (1:1,000). Individual data points are graphed on a log scale scatter plot with the means ± SEM and significance assessed by 2-tailed Student *t* test at $P < 0.05$ (NS, not significant).

Published OnlineFirst on July 19, 2012; DOI:10.1158/2159-8290.CD-12-0014

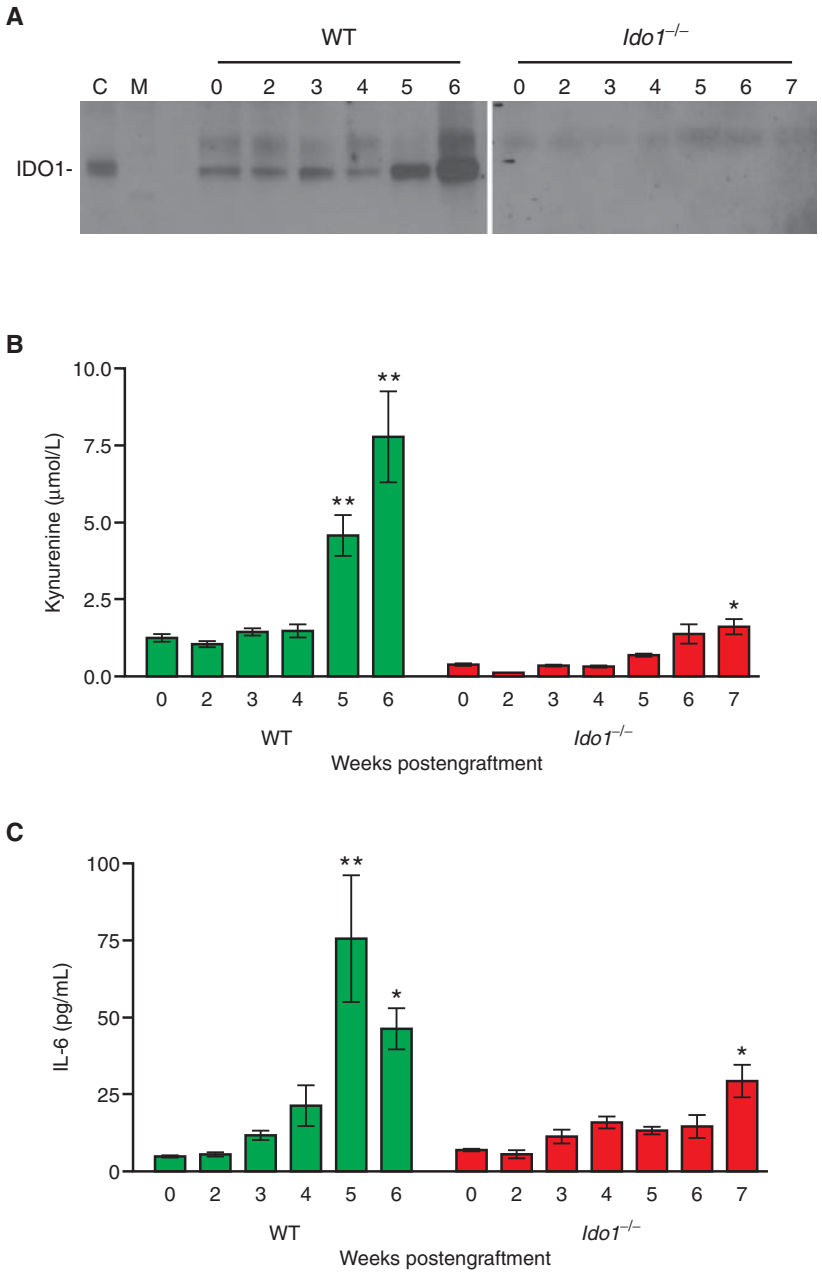

Figure 5. IDO deficiency is associated with attenuated induction of IL-6 during 4T1 tumor metastasis. **A,** evaluation of IDO1 protein levels by immunoprecipitation–Western blot analysis of lung tissue lysates from WT and *Ido1*$^{-/-}$ mice following orthotopic engraftment of 4T1 tumor cells at the time points in weeks indicated above each lane. C, epididymis lysate positive control lane; M, molecular weight marker lane. **B,** evaluation of kynurenine levels by LC/MS-MS–based analysis of homogenized lung samples from WT and *Ido1*$^{-/-}$ mice following orthotopic engraftment of 4T1 tumor cells at the time points in weeks indicted for each lane. Means ± SEM ($n \geq 6$) are graphed with significance relative to baseline determined by one-way ANOVA with Dunn test (*, $P < 0.05$; **, $P < 0.01$). **C,** IL-6 level determinations from cytokine bead array immunoassay–based analysis of homogenized lung samples from WT and *Ido1*$^{-/-}$ mice following orthotopic engraftment of 4T1 tumor cells at the time points in weeks indicted for each lane. Means ± SEM ($n \geq 3$) are graphed with significance relative to baseline determined by one-way ANOVA with Dunn test (*, $P < 0.05$; **, $P < 0.01$).

no difference in metastatic burden was observed in liver, although the presence of 4T1 cells was also nearly too low to detect in this tissue (Supplementary Fig. S2C). Because excision of the primary tumor can alter immune-based effects on metastasis (23), we evaluated the metastasis burden in resected mice. *Ido1*$^{-/-}$ mice continued to exhibit significant resistance to metastasis development (Fig. 4E), indicating that IDO-mediated support of metastatic development in lung is not dependent on the presence of the primary tumor. We also examined pulmonary VEGF levels but found that these increased comparably in both WT and *Ido1*$^{-/-}$ lungs during metastasis development and were actually somewhat higher at baseline in the *Ido1*$^{-/-}$ lungs (Supplementary Fig. S2D).

IDO Is Activated during Metastatic Lung Colonization and Potentiates IL-6 Induction

In WT mice, IDO1 protein and kynurenine levels both increased in the lungs during 4T1 metastasis development, particularly at 5 and 6 weeks postengraftment (Fig. 5A and B). The principal source of IDO1 expression in this context appears to be the native stroma rather than the engrafted 4T1 tumor cells because no IDO1 protein was detectable in the lungs of *Ido1*$^{-/-}$ mice (Fig. 5A), even at 7 weeks postengraftment when

Published OnlineFirst on July 19, 2012; DOI:10.1158/2159-8290.CD-12-0014

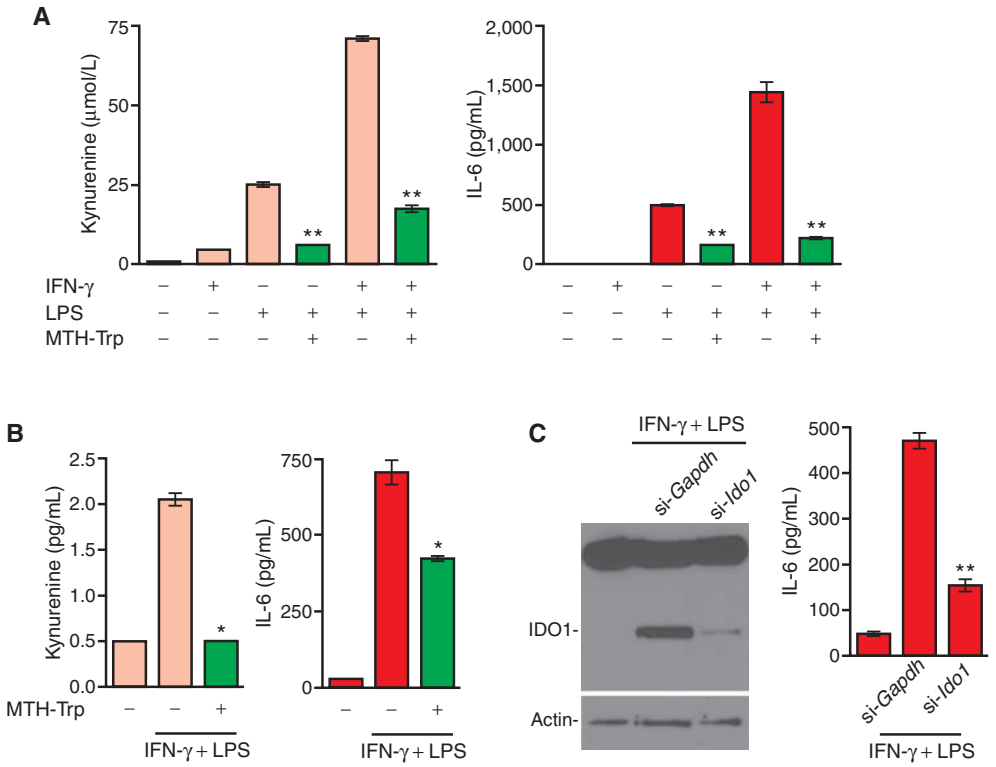

Figure 6. IDO-dependent potentiation of IL-6 production. **A,** supernatant from U937 cells stimulated for 24 hours with IFN-γ (100 ng/mL) and/or LPS (100 ng/mL) was analyzed for kynurenine and IL-6. Results from triplicate wells are plotted as the means ± SEM. Methylthiohydantoin tryptophan (MTH-Trp, 100 μmol/L) was included during induction where indicated and significance relative to the corresponding induced level without MTH-Trp was determined by 2-tailed Student *t* test (**, $P \leq 0.0001$). **B,** supernatant from HL-60 cells stimulated for 24 hours with IFN-γ (100 ng/mL) and LPS (100 ng/mL) was analyzed for kynurenine and IL-6. Results from duplicate wells are plotted as the means ± SEM. Methylthiohydantoin tryptophan (MTH-Trp, 100 μmol/L) was included during induction where indicated and significance relative to the corresponding induced level without MTH-Trp was determined by 2-tailed Student *t* test (*, $P < 0.05$). **C,** HL-60 cells treated in triplicate with *Ido1*-targeting (si-*Ido1*) or nontargeting (si-*Gapdh*) siRNAs were stimulated for 24 hours with IFN-γ (100 ng/mL) and LPS (100 ng/mL). Pooled cell lysates were analyzed by Western blot analysis for IDO1 and β-actin (left). IDO1 induction was suppressed by approximately 89.7% as assessed by densitometric analysis and normalization to actin. Individual cell supernatants were analyzed for IL-6 (right). The IL-6 data are plotted as the means ± SEM with the significance of the difference between specific *Ido1*-targeting versus nontargeting results determined by 2-tailed Student *t* test (**, $P < 0.0001$). *Gapdh*, glyceraldehyde-3-phosphate dehydrogenase.

the metastatic tumor burden was high. However, a weak but significant increase in kynurenine was observed in the lungs of *Ido1*$^{-/-}$ mice (Fig. 5B), suggesting that metastasis development may be associated with induction of an alternative mechanism of kynurenine production, such as IDO2 (24) or TDO2 (tryptophan 2,3-dioxygenase; ref. 25), either in conjunction with or in the absence of IDO1.

As in the *Kras*-driven primary lung tumor model, *Ido1* competence in the pulmonary metastatic setting was linked to enhanced elevation of IL-6, with levels increasing up to 15-fold over baseline in WT animals (Fig. 5C). On the other hand, the IL-6 levels in *Ido1*$^{-/-}$ lungs remained about 2- to 4-fold over baseline even when evaluated at an extended time point to account for the differential in tumor burden (Fig. 5C). Thus, like the autochthonous lung tumor studies, results from this lung metastasis model led us to infer a positive regulatory link between IDO and IL-6 production. Direct interrogation of this hypothesis was carried out in a cell-based assay with known IDO inducers. Lipopolysaccharide (LPS) induced both IDO activity and IL-6 production in monocytic U937 cells whereas IFN-γ on its own elicited little response but greatly elevated the level of IDO activity in combination with LPS that was mirrored by a comparable enhancement of IL-6 production (Fig. 6A). In both instances, inclusion of the competitive IDO-inhibitory compound MTH-tryptophan (8) significantly suppressed the observed increases in IDO activity as well as IL-6 production (Fig. 6A). MTH-tryptophan–mediated suppression of IL-6 induction was confirmed in a second monocytic cell line HL-60 (Fig. 6B). Likewise, siRNA-mediated interference with *Ido1* gene expression also significantly suppressed IL-6 induction (Fig. 6C). Taken together, these results are consistent with our *in vivo* findings suggesting that IDO activity can potentiate the elevated production of IL-6.

IDO Drives MDSC Expansion and Immunosuppressive Function

Studies in *Il1r*$^{-/-}$ (IL-1 receptor–nullizygous) mice have shown a crucial role for IL-6 in 4T1 pulmonary metastasis development (26). At the cellular level, IL-1β enhances development

Published OnlineFirst on July 19, 2012; DOI:10.1158/2159-8290.CD-12-0014

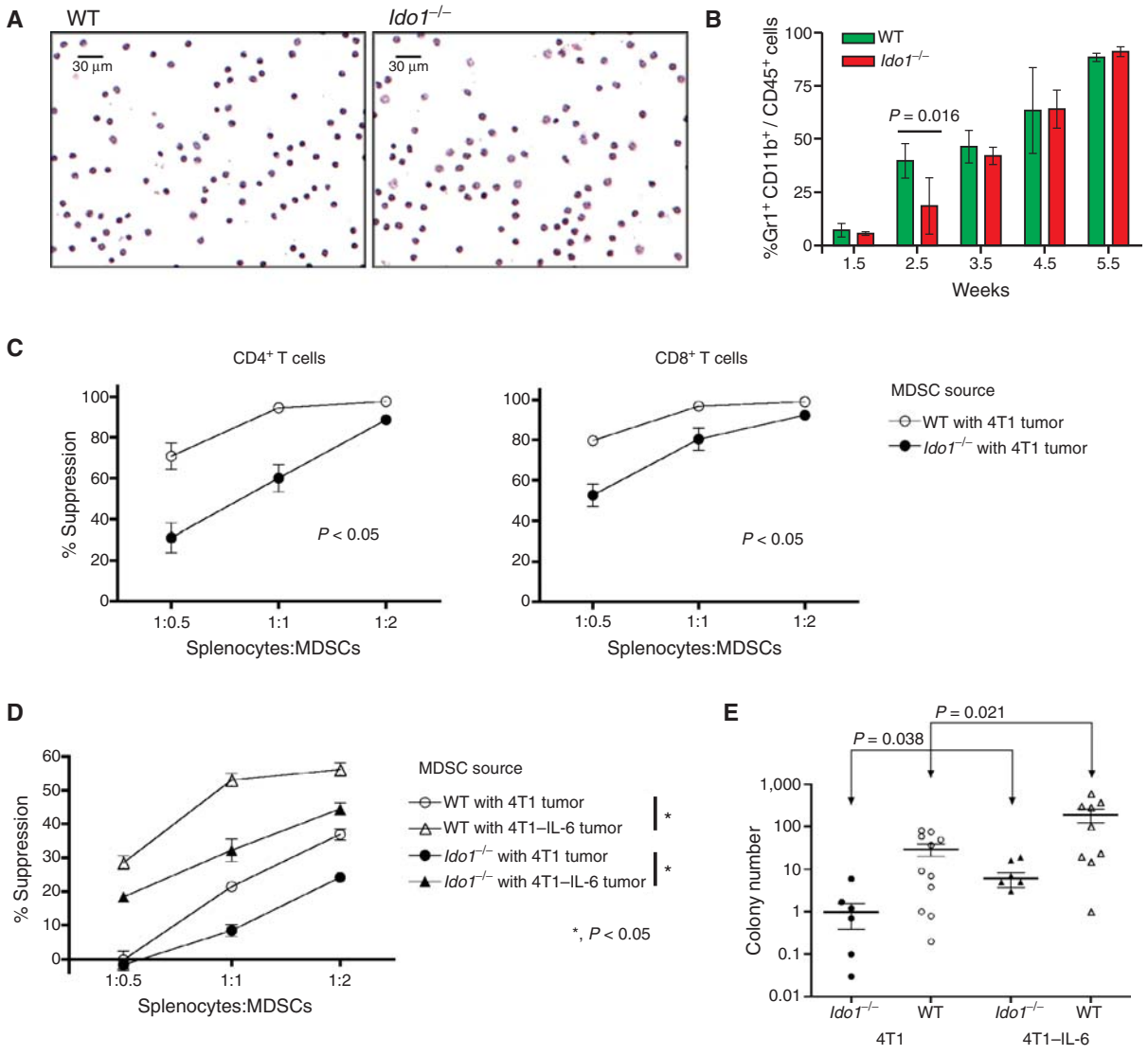

Figure 7. Attenuated MDSC-suppressive activity and metastasis development in IDO-deficient mice is rescued by IL-6. **A,** comparative microscopic images of hematoxylin and eosin (H&E)-stained MDSCs harvested from the blood of WT and *Ido1*$^{-/-}$ mice with primary 4T1 tumors that were not significantly different in size (12.2 ± 1.36 and 11. 5 ± 0.4 mm in diameter, respectively). **B,** single-cell suspensions of whole-lung tissues were prepared at the indicated time points following 4T1 engraftment into WT and *Ido1*$^{-/-}$ mice and evaluated by flow cytometry for MDSC infiltration by gating on CD45$^+$ cells and analyzing the Gr1$^+$ CD11b$^+$ cell population. Means ± SEM are graphed with significance assessed by 2-tailed Student *t* test at $P < 0.05$. **C,** splenocytes from CD4$^+$ TS1 (left) or CD8$^+$ Clone 4 (right) mice were cocultured in triplicate with cognate peptide and increasing proportions of 4T1-induced peripheral blood MDSCs from WT or *Ido1*$^{-/-}$ mice. T-cell activation was quantified by uptake of ^{3}H-thymidine and graphed as percentage of suppression relative to activation in the absence of MDSCs. Significance was assessed by Wilcoxon rank test at $P < 0.05$. Outcomes are representative of a minimum of 3 independent experiments. **D,** splenocytes from CD8$^+$ clone 4 transgenic mice were cocultured with cognate peptide and increasing proportions of 4T1 or 4T1-IL-6 tumor–induced MDSCs from WT or *Ido1*$^{-/-}$ mice for analysis as in **B.** Outcomes are representative of 6 independent experiments using TS1, clone 4, or DO11.10 transgenic T cells. **E,** colony-forming assays to assess the relative tumor cell burden in the lungs conducted 6 weeks following intravenous injection of 4T1 or 4T1-IL-6 cells into WT and *Ido1*$^{-/-}$ mice. Results are presented on log scale scatter plot with means ± SEM. Significance was assessed by 2-tailed Student *t* test at $P < 0.05$.

of tumor-promoting MDSCs with IL-6 serving as a critical downstream mediator of this process (26). Because *Ido1* loss attenuated IL-6 induction and metastatic colonization in the lung, we hypothesized that MDSCs may be compromised at some level in tumor-bearing *Ido1*$^{-/-}$ mice. MDSCs isolated from WT and *Ido1*$^{-/-}$ mice did not differ phenotypically (Fig. 7A; Supplementary Fig. S3A); however, an early delay in the expansion of Gr1$^+$CD11b$^+$ cells in *Ido1*$^{-/-}$ mice, similar to that observed in *Il1r*$^{-/-}$ animals (26), was noted (Fig. 7B). Moreover, circulating MDSCs isolated from *Ido1*$^{-/-}$ hosts were functionally impaired in their ability to suppress T cells (Fig. 7C). We did not detect IDO1 protein in Gr1$^+$CD11b$^+$ cells

obtained from tumor-bearing WT hosts (Supplementary Fig. S3B), consistent with the hypothesis that the observed functional impairment of MDSCs is a non–cell-autonomous effect of IDO deficiency in which IL-6 may act as a key intermediary.

IL-6 Is Critical to IDO-Driven MDSC Activity and Pulmonary Metastasis

To directly test the ability of IL-6 to functionally restore MDSC-suppressive activity in *Ido1*$^{-/-}$ mice, orthotopic tumors were established using 4T1–IL-6 cells (26), a 4T1 cell population engineered to constitutively express IL-6. MDSCs isolated from *Ido1*$^{-/-}$ mice engrafted with 4T1–IL-6 cells exhibited an elevated T-cell–suppressive activity similar to that of MDSCs isolated from WT hosts engrafted with parental 4T1 cells (Fig. 7D). Further enhancement of MDSC-suppressive activity could be achieved by engrafting 4T1–IL-6 cells into WT mice (Fig. 7D), indicating that the endogenous IL-6 levels stimulated by parental 4T1 tumor cells in WT animals were not fully saturating with regard to promoting MDSC suppressor function.

We next asked whether restoring IL-6 levels could also reverse the metastatic resistance exhibited by *Ido1*$^{-/-}$ mice. In the orthotopic setting, high levels of IL-6 produced in primary tumors formed by 4T1–IL-6 cells complicated the analysis by impairing the efficiency of pulmonary metastasis [possibly reflecting the recruitment of metastatic cancer cells back to IL-6–expressing primary tumors as documented previously (ref. 27)]. However, as our results in orthotopically engrafted mice had indicated that the *Ido1* allelic status does not affect 4T1 intravasation, we reasoned that a valid assessment of the impact of IDO deficiency on pulmonary metastasis could be made by introducing the metastatic tumor cells directly into the circulation. Accordingly, we confirmed that intravenously engrafted *Ido1*$^{-/-}$ mice maintained their resistance to pulmonary metastasis formation, with the apparent mean metastatic tumor burden being 30.4- and 31.6-fold lower in *Ido1*$^{-/-}$ versus WT mice challenged with 4T1 and 4T1–IL-6 cells, respectively (Fig. 7E). The proportional increase in metastatic burden observed in the 4T1–IL-6 challenged cohorts is also in line with the proposed interpretation of the MDSC functional data that IL-6 is not being produced at saturating levels in the 4T1-challenged WT animals. Because of the significantly higher metastasis burden produced by 4T1–IL-6 cells, comparison of 4T1–IL-6 challenged *Ido1*$^{-/-}$ mice to 4T1 challenged WT mice yielded a differential in mean metastatic tumor burden of only 4.8-fold (Fig. 7E). Thus, IL-6 supplementation not only rescued WT levels of MDSC suppressor function in 4T1 tumor-challenged *Ido1*$^{-/-}$ mice but also markedly restored their susceptibility to pulmonary metastasis development.

DISCUSSION

The idea of immune escape as a "hallmark of cancer" (28, 29) represents a groundbreaking although still largely untested paradigm within the field of cancer biology. The presumption that tumors exploit IDO activity as a mechanism of immune escape, initially inferred from the pioneering studies on maternal immune tolerance of Munn and colleagues (30), has become increasingly accepted despite a fundamental deficit in genetic support for the role of IDO in tumor development. This study addresses this gap with direct genetic validation of the importance of IDO in well-established models of lung cancer and metastasis that offers novel insights into the impact of IDO on tumor pathogenesis. Moreover, these findings strongly encourage the prioritization of clinical investigations into the use of IDO pathway inhibitors for treating lung adenocarcinomas and pulmonary metastases where more effective modalities are urgently needed.

While IDO activity was not elevated in lung tissue beyond baseline levels during KRAS-driven lung tumor development, the observed reduction in pulmonary vascularization in *Ido1*$^{-/-}$ animals even before initiation of tumorigenesis implied that the loss of steady-state IDO in this context was sufficiently consequential to impact physiologic processes important to tumor outgrowth. Enhanced tumor vascularization has been reported in tumor xenograft models involving exogenous IDO overexpression (31,32), but our study is the first to identify a role for IDO in supporting vascular development under native physiologic conditions. Our findings likewise genetically establish the importance of IDO activity in nontumor cells for supporting pulmonary metastasis. In this manner, IDO activity may influence metastatic dissemination to tissues such as the lung where its expression is particularly robust. This may, however, be less relevant when IDO [or tryptophan 2,3-dioxygenase (ref. 25)] activity is substantially elevated within the tumor cells themselves (8, 33), enabling the malignancy to preemptively shape its surroundings through intrinsic tryptophan catabolism. As such, IDO activity that originates from stromal cells of the tumor microenvironment or from the tumor cells themselves may contribute to directing tumor outgrowth.

The positive association between IDO and IL-6 in lung tumorigenesis and metastasis was not necessarily anticipated, given that it runs counter to expectations based on IDO-mediated induction of liver-enriched inhibitory protein (LIP), a negative regulatory isoform of the *Il6* gene expression promoting transcription factor C/EBPβ (24, 34). The precise regulatory impact of LIP on *Il6* expression is not clear cut, however, insofar as other findings have indicated that LIP can interact with NF-κB to induce rather than limit *Il6* transcription (35). Our findings are also consistent with evidence that a downstream product of IDO-mediated catabolism, kynurenic acid, can potentiate IL-6 production in the context of inflammation by signaling through the aryl hydrocarbon receptor (36). IL-6 is a pleiotropic cytokine that is widely implicated in supporting neoplastic outgrowth in the context of chronic inflammation (37). Clinically, IL-6 has been established as a marker of early relapse of resected lung tumors (38). Analyses of DNA polymorphisms in the IL-6 promoter region have identified positive correlations between IL-6 inducibility and lung cancer susceptibility in the context of concurrent inflammatory disease (39) as well as micrometastatic disease in patients with high-risk breast cancer (40). Functionally, IL-6 induction has been identified as an essential downstream component of RAS-induced tumorigenesis (41) that is directly linked to lung tumor development in the *Lox-Kras*^{G12D} transgenic mouse model (21). Numerous other studies indicate that IL-6 can also contribute to tumor promotion by supporting angiogenesis and neovascularization of tumors (42, 43). Thus, biologically,

Published OnlineFirst on July 19, 2012; DOI:10.1158/2159-8290.CD-12-0014

the epidemiologic and functional data for IL-6 are consistent with the tumor-promoting activity that we have ascribed to IDO through mouse genetics.

Tumor responses to IDO-inhibitory compounds require functional host immunity (5, 6, 8, 9), but the mechanisms through which IDO promotes immune escape have yet to be fully delineated. Connecting IL-6 to IDO provides valuable insight in this regard. IL-6 has previously been identified in the 4T1 metastasis model as critical to the induction of MDSCs, which act as potent inhibitors of antitumor immunity (44). MDSC accumulation is known to be driven by several factors that are produced by tumor cells and the tumor stroma, including the potent inflammatory mediators prostaglandin E2 and IL-1β (45–47). Genetic ablation of IL-1β signaling can affect both the early accumulation of MDSCs as well as their immunosuppressive capability (26), and IL-6 has been determined to be a downstream mediator for the effects of IL-1β on MDSC populations in tumor-bearing animals (26). In this context, our findings identify IDO as a key determinant of IL-6–elicited MDSC accumulation and suppressor activity. Interestingly, IL-1β may dynamically potentiate the contribution of IDO to IL-6 induction given that IL-1β can promote the upregulation of IFNGR1 (48) that enhances *Ido1* inducibility in response to IFN-γ. In contrast, IL-6 may exert a counter-regulatory feedback effect by inducing SOCS3 (suppressor of cytokine signaling 3), which not only attenuates IL-6 signaling (49) but also limits IDO transcription and IDO enzyme stability (50, 51). Thus, IDO is well situated to act as a dynamic modifier of inflammatory states in the microenvironment of primary tumors or budding metastases.

Our results deepen the concept that IDO activity profoundly influences the pathogenic character of the tumor microenvironment by identifying the cytokine IL-6 as a crucial IDO effector for establishing "cancer-associated" inflammation. IL-6 is a far-reaching, pleiotropic signaling molecule that can elicit both intrinsic and extrinsic effects on tumor development (i.e., increased malignancy and survival as well as increased angiogenesis and immune escape). The ramifications of our results thus extend beyond the constrained effects that local IDO-mediated tryptophan catabolism might exert on the proximal microenvironment, and one would expect the potentiation of IL-6 expression by IDO to affect diverse aspects of tumor development with the relative weighting of each aspect being an important focus of future study. Indeed, further investigations of IDO as a nexus for control of tumorigenic inflammation, vascularization, and immune escape will be invaluable in formulating rational strategies to guide the best application of IDO inhibitors that have entered clinical development.

METHODS

Transgenic Mouse Strains

Congenic *Ido1*$^{-/-}$ mice on C57BL/6 and BALB/c strain backgrounds were provided by A. Mellor (Georgia Health Sciences University, GSHU, Augusta GA), and corresponding control strains were purchased from Jackson Laboratory. *LSL-Kras*^{G12D} *Cre*-inducible transgenic mice on a mixed 129SvJ-C57BL/6 strain background (16) were obtained through the Mouse Models of Human Cancer Consortium (NCI-Frederick, Frederick, MD). Administration of Ad-*Cre* virus to activate the latent *Kras*^{G12D} allele in lungs of *LSL-Kras*^{G12D} transgenic mice (referred to as *Lox-Kras*^{G12D} mice; ref. 16) was carried out as described (52). Doubly mutant *Ido1*$^{-/-}$ *LSL-Kras*^{G12D} mice were generated through breeding of the 2 transgenic strains. Mating pairs of BALB/c and T-cell receptor (TcR) transgenic DO11.10 BALB/c mice (I-A^{d}–restricted, specific for chicken ovalbumin$_{323–339}$) were obtained from The Jackson Laboratory. Mating pairs of TcR transgenic Clone 4 BALB/c mice [H-2K^{d}–restricted, specific to influenza hemagglutinin (HA) peptide$_{518–526}$] and TcR transgenic TS1 BALB/c mice (I-E^{d}–restricted, specific to HA peptide$_{110–119}$) were provided by E. Fuchs (Johns Hopkins, Baltimore, MD). All procedures involving mice were approved by either the Lankenau Institute for Medical Research (LIMR; Wynnewood, PA) or University of Maryland Baltimore County (UMBC) Institutional Animal Care and Use Committee (IACUC).

Micro-CT Scanning

Three-dimensional micro-CT images were acquired from anesthetized mice using an Impek Micro-CT scanner operated at 40-kVp, 500-μA, 250-millisecond per frame, 5 frames per view, 360 views, and 1-degree increments per view. Contiguous axial DICOM-formatted images through each mouse thorax, with voxels of dimensions 91 μm × 91 μm × 91 μm were compiled into 3D format using Amira v5.1 software and normalized to Hounsfield units. Using the segmentation editor, manual selections of the chest cavity minus the heart were conducted on every other slice followed by interpolation of these selections. Magic wand tool selection was conducted at the threshold range defining air (determined to be between −750 and −350) to define the functional lung volume, which was automatically subtracted from the total chest space to identify the volume representing vasculature and tumors (20).

4T1 Tumor Cell Metastasis

Parental 4T1 mouse mammary carcinoma cells and 4T1-derived cell lines expressing luciferase (4T1-luc) or mouse *Il6* (4T1–IL-6) were maintained as described (5, 22, 26). Primary tumor growth was monitored by caliper measurements of orthogonal diameters. Tumor volume was calculated using the formula for determining a prolapsed elliptoid $[(d^2 \times l)/0.52]$, where d is the shorter of the 2 orthogonal measurements. To enhance visualization of metastatic nodules, lungs were insufflated with India ink dye, washed, and bleached in Fekete's solution. The clonogenic assay to assess metastatic burden was conducted as described (22).

Real-time PCR

Lung DNA was analyzed by Real Time-PCR containing SYBR green PCR master mix (Applied Biosystems) and primers to amplify *Cre* (5′-GGAGCCGCGCGAGATA-3′ and 5′-GCCACCAGCTTGCATGATC-3′) and endogenous mouse *Cd81* (5′-TCGCCAAGGATGTGAAGCA-3′ and 5′-CATTGTTGGCATCATCATCCA-3′). Assays were conducted in quadruplicate, and relative quantitation of the viral *Cre* gene present in lung tissue was calculated using the comparative threshold cycle (C_T) method (User Bulletin 2, Applied Biosystems) normalizing the target C_T values to the internal housekeeping gene (*Cd81*).

Histology

Tissues were isolated and fixed in 10% neutral-buffered formalin or 4% paraformaldehyde, sectioned, and stained for histopathologic analysis with hematoxylin and eosin using standard methods. For immunofluorescent staining, 4-μm paraffin sections were deparaffinized in xylene and rehydrated with a graded alcohol series. Following antigen retrieval (vector), sections were washed and placed in 0.1% Triton for 10 minutes. Tissue was blocked in 40 μg/mL goat anti-mouse IgG-Fab (H+L) (Jackson ImmunoResearch) followed by

Published OnlineFirst on July 19, 2012; DOI:10.1158/2159-8290.CD-12-0014

10% normal goat serum (Jackson ImmunoResearch). Rabbit anti-mouse caveolin-1 (1:200; Cell Signaling) was incubated overnight at 4°C. Sections were washed and incubated with goat anti-rabbit Cy3 (1:200; Jackson ImmunoResearch). Tissues were mounted using Prolong Gold with DAPI (Invitrogen). To quantitate the blood vessel areas present within defined fields of caveolin-1–stained lung samples, 4 images were acquired per mouse from 5 WT and 5 *Ido1*$^{-/-}$ mice. Vessel boundaries were identified by caveolin-1 staining, and the area of every vessel within each field was determined using AxioVision Release 4.6 software.

Immunoprecipitation–Western Blot Analysis

Immunoprecipitation of IDO1 protein from mouse lung tissue with purified rabbit polyclonal antibody (7) followed by Western blotting–based detection with rat monoclonal antibody (clone mIDO-48; BioLegend) was carried out as described (9).

Flow Cytometry for Cytokine and Cell Analysis

Flow cytometric data were acquired on a FACSCanto II or Cyan ADP flow cytometer and analyzed using FACSDIVA (BD Biosciences) or Summit v4.3.02 (Beckman/Coulter) software. Multiplexed cytokine analysis was conducted using the Inflammation Bead Array (BD Biosciences). Lung homogenates were centrifuged and supernatant added to beads in the array according to the manufacturer's instructions. Flow cytometric analysis of MDSCs harvested from digested lung samples or from blood was conducted with the following antibodies as indicated: Gr1-FITC, Ly6G-PE, Ly6C-FITC, and CD124 (IL-4Rα)-PE (BD Biosciences); CD11b-PacB, CD115-PE, and F4/80-PE (BioLegend); Ly6C-PerCP (eBioscience); and arginase and iNOS (BD Transduction Labs). Second step goat anti-mouse IgG-Alexa 647 for arginase and inducible NO synthase (iNOS) was from Invitrogen. Isotype control antibodies were from BD Biosciences.

Kynurenine Assay

Lungs were homogenized in PBS containing dithiothreitol (DTT) and protease and phosphatase inhibitors (1:3 wt/vol). Deproteinated lysates were analyzed by high-performance liquid chromatography (HPLC) coupled to electrospray ionization liquid chromatography/tandem mass spectroscopy (LC/MS-MS) analysis as described (9).

Cell Culture

U937 and HL-60 monocytic cell lines (American Type Culture Collection) were expanded for frozen storage after receipt and freshly thawed cells cultured in Dulbecco's Modified Eagle's Media + 10% FBS were used at early passage for experiments. No additional authentication was conducted by the authors. Twenty-four–hour treatment of cells with LPS (100 ng/mL; Sigma) and/or IFN-γ (100 ng/mL; R&D systems) was carried out in triplicate on 1×10^4 cells per well in a 96-well dish. MTH-Trp (methylthiohydantoin-DL-tryptophan; 100 μmol/L; Sigma) was also included at the time of induction as indicated. Kynurenine and IL-6 levels in the supernatant were analyzed as described above. *Ido1* gene "knockdown" studies were conducted with siRNAs (Dharmacon) targeting *Ido1* (catalog no. E-010337-00) or *Gapdh* (catalog no. D-001930-01) using the Accell siRNA Delivery System (Dharmacon) as described by the manufacturer. HL-60 cells were plated at 1×10^4 per well in a 96-well dish and cultured with 1% FBS in the Accell growth media. Twenty-four–hour treatment of cells with LPS and IFN-γ was initiated at 48 hours following incubation with siRNA. Western blotting to detect IDO1 protein in cell lysates was conducted following standard procedures using rabbit polyclonal anti-IDO1 (7) and rabbit monoclonal anti-β-actin (13E5; Cell Signaling) as a loading control. Detection was carried out with goat anti-rabbit IgG, horseradish peroxidase (HRP)-linked secondary antibody (catalog no. 7074; Cell Signaling) using the SuperSignal West Femto Chemiluminescent substrate (Thermo Scientific).

T-cell Suppression Assay

MDSC-suppressive activity was measured as previously described (53) using transgenic splenocytes and their cognate peptides in the presence of 25 Gy–irradiated, blood-derived MDSCs from 4T1 tumor–bearing mice. $HA_{518-526}$, $HA_{110-119}$, and $Ova_{323-339}$ peptides were synthesized in the Biopolymer Core Facility at the University of Maryland, Baltimore, MD. ELISA duo set mAbs for mIL6 were from R&D Systems. Monoclonal antibody Vβ8.1,8.2-PE was from BD PharMingen.

Disclosure of Potential Conflicts of Interest

G.C. Prendergast, A.J. Muller, and J.B. DuHadaway declare a potential conflict of interest with regard to IDO due to intellectual property, financial interests, grant support, and consultancy roles with New Link Genetics Corporation, which is engaged in the clinical development of IDO inhibitors for the purpose of treating cancer and other diseases. R. Metz is an employee of New Link Genetics Corporation as Director of Research and has financial and intellectual property interests in the company. No potential conflicts of interests were disclosed by the other authors.

Authors' Contributions

Conception and design: C. Smith, S. Ostrand-Rosenberg, G.C. Prendergast, A.J. Muller

Development of methodology: C. Smith, J.B. DuHadaway, L.D. Laury-Kleintop, L. Mandik-Nayak, R. Metz, S. Ostrand-Rosenberg, A.J. Muller

Acquisition of data (provided animals, acquired and managed patients, provided facilities, etc.): C. Smith, M.Y. Chang, K.H. Parker, D.W. Beury, J.B. DuHadaway, J. Boulden, E. Sutanto-Ward, S. Ostrand-Rosenberg

Analysis and interpretation of data (e.g., statistical analysis, biostatistics, computational analysis): C. Smith, M.Y. Chang, K.H. Parker, D.W. Beury, H.E. Flick, A.P. Soler, L.D. Laury-Kleintop, L. Mandik-Nayak, S. Ostrand-Rosenberg, G.C. Prendergast, A.J. Muller

Writing, review, and/or revision of the manuscript: C. Smith, D.W. Beury, A.P. Soler, L.D. Laury-Kleintop, L. Mandik-Nayak, R. Metz, S. Ostrand-Rosenberg, G.C. Prendergast, A.J. Muller

Administrative, technical, or material support (i.e., reporting or organizing data, constructing databases): C. Smith, J. Boulden, A.P. Soler, S. Ostrand-Rosenberg

Study supervision: C. Smith, S. Ostrand-Rosenberg, A.J. Muller, G.C. Prendergast

Acknowledgments

The authors thank Gwen Guillard for tissue sectioning and histology and Lingling Yang for preliminary studies on MDSCs in IDO-deficient mice.

Grant Support

A.J. Muller is the recipient of grants from Susan G. Komen for the Cure and the W.W. Smith Foundation. G.C. Prendergast is the recipient of NIH grants CA109542, CA159337, and CA159315 with additional support from NewLink Genetics Corporation, the Sharpe-Strumia Foundation, the Lankenau Medical Center Foundation, and the Main Line Health System. S. Ostrand-Rosenberg is the recipient of NIH grants RO1CA115880, RO1CA84232, and RO1GM021248. C. Smith is the recipient of a postdoctoral fellowship through the Department of Defense Breast Cancer Research Program. D. Beury is the recipient of a predoctoral fellowship through the Department of Defense Breast Cancer Research Program.

Received January 12, 2012; revised May 31, 2012; accepted June 1, 2012; published OnlineFirst July 19, 2012.

REFERENCES

1. Peek RM Jr, Mohla S, DuBois RN. Inflammation in the genesis and perpetuation of cancer: summary and recommendations from a national cancer institute-sponsored meeting. Cancer Res 2005;65:8583–6.
2. Muller AJ, Mandik-Nayak L, Prendergast GC. Beyond immunosuppression: reconsidering indoleamine 2,3-dioxygenase as a pathogenic element of chronic inflammation. Immunotherapy 2010;2:293–7.
3. Muller AJ, Scherle PA. Targeting the mechanisms of tumoral immune tolerance with small-molecule inhibitors. Nat Rev Cancer 2006; 6:613–25.
4. Banerjee T, DuHadaway JB, Gaspari P, Sutanto-Ward E, Munn DH, Mellor AL, et al. A key *in vivo* antitumor mechanism of action of natural product-based brassinins is inhibition of indoleamine 2,3-dioxygenase. Oncogene 2008;27:2851–7.
5. Hou DY, Muller AJ, Sharma MD, DuHadaway J, Banerjee T, Johnson M, et al. Inhibition of indoleamine 2,3-dioxygenase in dendritic cells by stereoisomers of 1-methyl-tryptophan correlates with antitumor responses. Cancer Res 2007;67:792–801.
6. Kumar S, Malachowski WP, Duhadaway JB, Lalonde JM, Carroll PJ, Jaller D, et al. Indoleamine 2,3-dioxygenase is the anticancer target for a novel series of potent naphthoquinone-based inhibitors. J Med Chem 2008;51:1706–18.
7. Metz R, Duhadaway JB, Rust S, Munn DH, Muller AJ, Mautino M, et al. Zinc protoporphyrin IX stimulates tumor immunity by disrupting the immunosuppressive enzyme indoleamine 2,3-dioxygenase. Mol Cancer Ther 2010;9:1864–71.
8. Muller AJ, Duhadaway JB, Donover PS, Sutanto-Ward E, Prendergast GC. Inhibition of indoleamine 2,3-dioxygenase, an immunoregulatory target of the cancer suppression gene Bin1, potentiates cancer chemotherapy. Nat Med 2005;11:312–9.
9. Muller AJ, DuHadaway JB, Jaller D, Curtis P, Metz R, Prendergast GC. Immunotherapeutic suppression of indoleamine 2,3-dioxygenase and tumor growth with ethyl pyruvate. Cancer Res 2010;70:1845–53.
10. Koblish HK, Hansbury MJ, Bowman KJ, Yang G, Neilan CL, Haley PJ, et al. Hydroxyamidine inhibitors of indoleamine-2,3-dioxygenase potently suppress systemic tryptophan catabolism and the growth of IDO-expressing tumors. Mol Cancer Ther 2010;9:489–98.
11. Balachandran VP, Cavnar MJ, Zeng S, Bamboat ZM, Ocuin LM, Obaid H, et al. Imatinib potentiates antitumor T cell responses in gastrointestinal stromal tumor through the inhibition of Ido. Nat Med 2011;17:1094–100.
12. Muller AJ, Duhadaway JB, Chang MY, Ramalingam A, Sutanto-Ward E, Boulden J, et al. Non-hematopoietic expression of IDO is integrally required for inflammatory tumor promotion. Cancer Immunol Immunother 2010;59:1655–63.
13. Muller AJ, Sharma MD, Chandler PR, Duhadaway JB, Everhart ME, Johnson BA III, et al. Chronic inflammation that facilitates tumor progression creates local immune suppression by inducing indoleamine 2,3 dioxygenase. Proc Natl Acad Sci U S A 2008; 105:17073–8.
14. Yoshida R, Imanishi J, Oku T, Kishida T, Hayaishi O. Induction of pulmonary indoleamine 2,3-dioxygenase by interferon. Proc Natl Acad Sci U S A 1981;78:129–32.
15. Yoshida R, Urade Y, Tokuda M, Hayaishi O. Induction of indoleamine 2,3-dioxygenase in mouse lung during virus infection. Proc Natl Acad Sci U S A 1979;76:4084–6.
16. Jackson EL, Willis N, Mercer K, Bronson RT, Crowley D, Montoya R, et al. Analysis of lung tumor initiation and progression using conditional expression of oncogenic K-ras. Genes Dev 2001;15:3243–8.
17. Ji H, Houghton AM, Mariani TJ, Perera S, Kim CB, Padera R, et al. K-ras activation generates an inflammatory response in lung tumors. Oncogene 2006;25:2105–12.
18. Baban B, Chandler P, McCool D, Marshall B, Munn DH, Mellor AL. Indoleamine 2,3-dioxygenase expression is restricted to fetal trophoblast giant cells during murine gestation and is maternal genome specific. J Reprod Immunol 2004;61:67–77.
19. Ozaki Y, Edelstein MP, Duch DS. Induction of indoleamine 2,3-dioxygenase: a mechanism of the antitumor activity of interferon gamma. Proc Natl Acad Sci U S A 1988;85:1242–6.
20. Haines BB, Bettano KA, Chenard M, Sevilla RS, Ware C, Angagaw MH, et al. A quantitative volumetric micro-computed tomography method to analyze lung tumors in genetically engineered mouse models. Neoplasia 2009;11:39–47.
21. Ochoa CE, Mirabolfathinejad SG, Ruiz VA, Evans SE, Gagea M, Evans CM, et al. Interleukin 6, but not T helper 2 cytokines, promotes lung carcinogenesis. Cancer Prev Res (Phila) 2011;4:51–64.
22. Pulaski BA, Ostrand-Rosenberg S. Mouse 4T1 breast tumor model. In: Coligan JE, Kruisbeek AM, Margulies DH, Shevach EM, Strober W, editors. Current protocols in immunology. New York: John Wiley & Sons, Inc.; 2000. p. 20.2.1–16.
23. Ostrand-Rosenberg S, Clements VK, Terabe M, Park JM, Berzofsky JA, Dissanayake SK. Resistance to metastatic disease in STAT6-deficient mice requires hemopoietic and nonhemopoietic cells and is IFN-gamma dependent. J Immunol 2002;169:5796–804.
24. Metz R, Duhadaway JB, Kamasani U, Laury-Kleintop L, Muller AJ, Prendergast GC. Novel tryptophan catabolic enzyme IDO2 is the preferred biochemical target of the antitumor indoleamine 2,3-dioxygenase inhibitory compound D-1-methyl-tryptophan. Cancer Res 2007;67:7082–7.
25. Opitz CA, Litzenburger UM, Sahm F, Ott M, Tritschler I, Trump S, et al. An endogenous tumour-promoting ligand of the human aryl hydrocarbon receptor. Nature 2011;478:197–203.
26. Bunt SK, Yang L, Sinha P, Clements VK, Leips J, Ostrand-Rosenberg S. Reduced inflammation in the tumor microenvironment delays the accumulation of myeloid-derived suppressor cells and limits tumor progression. Cancer Res 2007;67:10019–26.
27. Kim MY, Oskarsson T, Acharyya S, Nguyen DX, Zhang XH, Norton L, et al. Tumor self-seeding by circulating cancer cells. Cell 2009;139:1315–26.
28. Luo J, Solimini NL, Elledge SJ. Principles of cancer therapy: oncogene and non-oncogene addiction. Cell 2009;136:823–37.
29. Prendergast GC. Immune escape as a fundamental trait of cancer: focus on IDO. Oncogene 2008;27:3889–900.
30. Munn DH, Zhou M, Attwood JT, Bondarev I, Conway SJ, Marshall B, et al. Prevention of allogeneic fetal rejection by tryptophan catabolism. Science 1998;281:1191–93.
31. Nonaka H, Saga Y, Fujiwara H, Akimoto H, Yamada A, Kagawa S, et al. Indoleamine 2,3-dioxygenase promotes peritoneal dissemination of ovarian cancer through inhibition of natural killer cell function and angiogenesis promotion. Int J Oncol 2011;38:113–20.
32. Li Y, Tredget EE, Ghaffari A, Lin X, Kilani RT, Ghahary A. Local expression of indoleamine 2,3-dioxygenase protects engraftment of xenogeneic skin substitute. J Invest Dermatol 2006;126:128–36.
33. Uyttenhove C, Pilotte L, Theate I, Stroobant V, Colau D, Parmentier N, et al. Evidence for a tumoral immune resistance mechanism based on tryptophan degradation by indoleamine 2,3-dioxygenase. Nat Med 2003;9:1269–74.
34. Sharma MD, Hou DY, Liu Y, Koni PA, Metz R, Chandler P, et al. Indoleamine 2,3-dioxygenase controls conversion of Foxp3+ Tregs to TH17-like cells in tumor-draining lymph nodes. Blood 2009;113:6102–11.
35. Hu HM, Tian Q, Baer M, Spooner CJ, Williams SC, Johnson PF, et al. The C/EBP bZIP domain can mediate lipopolysaccharide induction of the proinflammatory cytokines interleukin-6 and monocyte chemoattractant protein-1. J Biol Chem 2000;275:16373–81.

36. DiNatale BC, Murray IA, Schroeder JC, Flaveny CA, Lahoti TS, Laurenzana EM, et al. Kynurenic acid is a potent endogenous aryl hydrocarbon receptor ligand that synergistically induces interleukin-6 in the presence of inflammatory signaling. Toxicol Sci 2010;115:89–97.
37. Hodge DR, Hurt EM, Farrar WL. The role of IL-6 and STAT3 in inflammation and cancer. Eur J Cancer 2005;41:2502–12.
38. Kita H, Shiraishi Y, Watanabe K, Suda K, Ohtsuka K, Koshiishi Y, et al. Does postoperative serum interleukin-6 influence early recurrence after curative pulmonary resection of lung cancer? Ann Thorac Cardiovasc Surg 2011;17:454–60.
39. Seow A, Ng DP, Choo S, Eng P, Poh WT, Ming T, et al. Joint effect of asthma/atopy and an IL-6 gene polymorphism on lung cancer risk among lifetime non-smoking Chinese women. Carcinogenesis 2006;27:1240–4.
40. DeMichele A, Martin AM, Mick R, Gor P, Wray L, Klein-Cabral M, et al. Interleukin-6 -174G->C polymorphism is associated with improved outcome in high-risk breast cancer. Cancer Res 2003;63:8051–6.
41. Ancrile B, Lim KH, Counter CM. Oncogenic Ras-induced secretion of IL6 is required for tumorigenesis. Genes Dev 2007;21:1714–9.
42. Angelo LS, Kurzrock R. Vascular endothelial growth factor and its relationship to inflammatory mediators. Clin Cancer Res 2007;13:2825–30.
43. Grivennikov SI, Karin M. Inflammatory cytokines in cancer: tumour necrosis factor and interleukin 6 take the stage. Ann Rheum Dis 2011;70 Suppl 1: i104–8.
44. Ostrand-Rosenberg S, Sinha P. Myeloid-derived suppressor cells: linking inflammation and cancer. J Immunol 2009;182:4499–506.
45. Bunt SK, Sinha P, Clements VK, Leips J, Ostrand-Rosenberg S. Inflammation induces myeloid-derived suppressor cells that facilitate tumor progression. J Immunol 2006;176:284–90.
46. Sinha P, Clements VK, Fulton AM, Ostrand-Rosenberg S. Prostaglandin E2 promotes tumor progression by inducing myeloid-derived suppressor cells. Cancer Res 2007;67:4507–13.
47. Song X, Krelin Y, Dvorkin T, Bjorkdahl O, Segal S, Dinarello CA, et al. CD11b+/Gr-1+ immature myeloid cells mediate suppression of T cells in mice bearing tumors of IL-1beta-secreting cells. J Immunol 2005;175:8200–8.
48. Shirey KA, Jung JY, Maeder GS, Carlin JM. Upregulation of IFN-gamma receptor expression by proinflammatory cytokines influences IDO activation in epithelial cells. J Interferon Cytokine Res 2006;26:53–62.
49. Heinrich PC, Behrmann I, Haan S, Hermanns HM, Muller-Newen G, Schaper F. Principles of interleukin (IL)-6-type cytokine signalling and its regulation. Biochem J 2003;374:1–20.
50. Orabona C, Belladonna ML, Vacca C, Bianchi R, Fallarino F, Volpi C, et al. Cutting edge: silencing suppressor of cytokine signaling 3 expression in dendritic cells turns CD28-Ig from immune adjuvant to suppressant. J Immunol 2005;174:6582–6.
51. Orabona C, Pallotta MT, Volpi C, Fallarino F, Vacca C, Bianchi R, et al. SOCS3 drives proteasomal degradation of indoleamine 2,3-dioxygenase (IDO) and antagonizes IDO-dependent tolerogenesis. Proc Natl Acad Sci U S A 2008;105:20828–33.
52. Fasbender A, Lee JH, Walters RW, Moninger TO, Zabner J, Welsh MJ. Incorporation of adenovirus in calcium phosphate precipitates enhances gene transfer to airway epithelia *in vitro* and *in vivo*. J Clin Invest 1998;102:184–93.
53. Sinha P, Clements VK, Ostrand-Rosenberg S. Reduction of myeloid-derived suppressor cells and induction of M1 macrophages facilitate the rejection of established metastatic disease. J Immunol 2005;174:636–45.

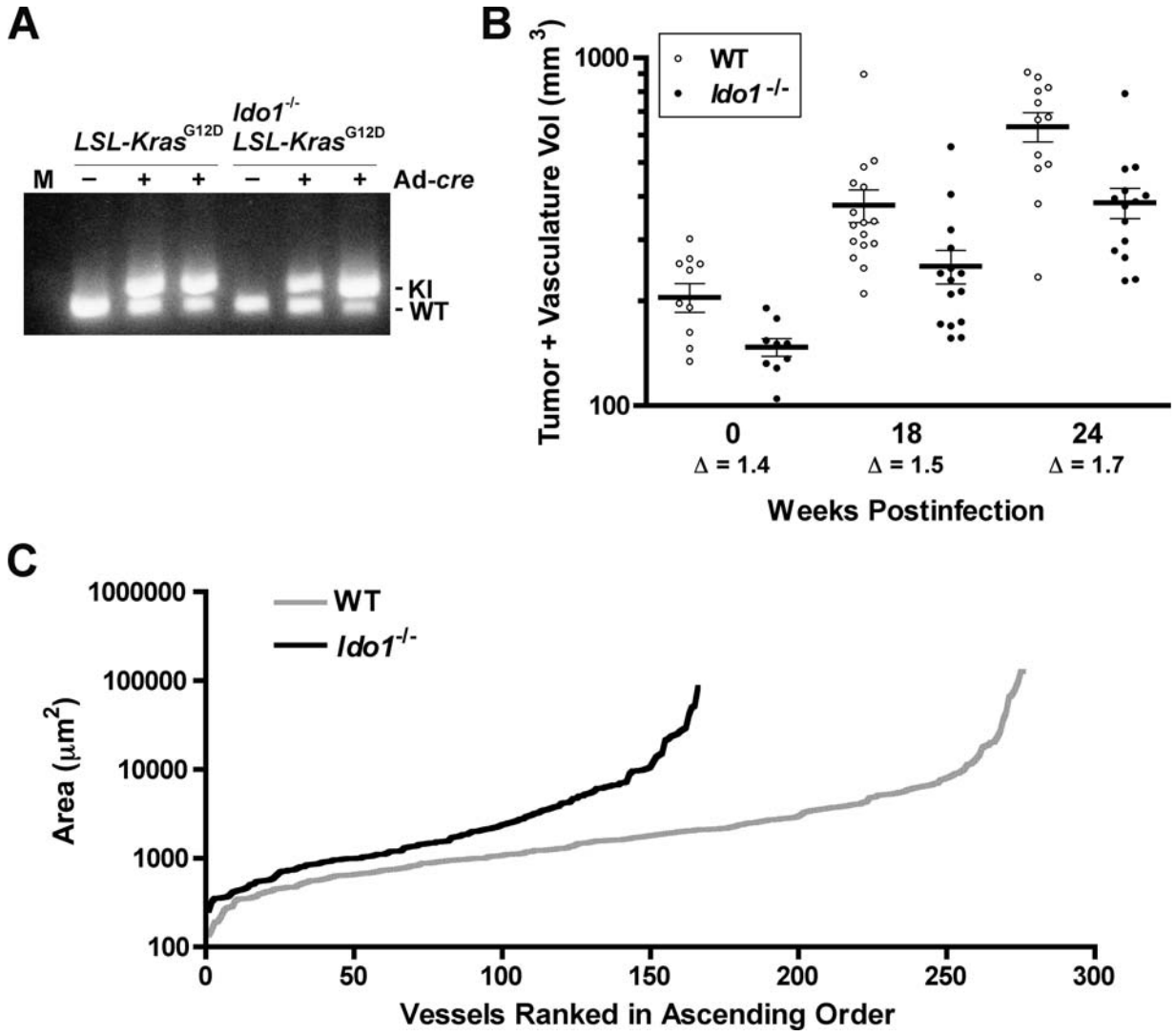

Supplementary Figure S1. (**A**) Confirmation of the presence of the recombined *Lox-Kras*^{G12D} allele in Ad-*cre* infected mice with lung tumors. PCR-based analysis of genomic DNA prepared from lung tissue from *LSL-Kras*^{G12D} and *Ido1*$^{-/-}$ *LSL-Kras*^{G12D} mice prior to infection (–) and from 2 mice from each group at 26wk postinfection (+). The recombined *Lox-Kras*^{G12D} knockin (KI) allele yields a product of 315 bp evident only in the post-infection lanes, while the opposite, unmodified (WT) *Kras* allele yields a product of 285 bp present in every lane. The silenced, non-recombined *LSL-Kras*^{G12D} knockin allele is too large to be detected in this assay. The marker (M) is HaeIII digested φX174 phage DNA. (**B**) The difference in tumor and vasculature volumes

between mice with and without IDO is proportionately similar even prior to the onset of tumor development. To graphically demonstrate the proportionality of the differences in pulmonary tumor and vasculature volumes between *LSL-Kras*^{G12D} and *Ido1*$^{-/-}$ *LSL-Kras*^{G12D} mice at the 0, 18 and 24 week time points, the data presented in Figure 2B are plotted on a log scale. The data are graphed as a scatter plot with bars representing the means ± SE. The fold difference (Δ) between the mean calculated tumor and vasculature volumes for the two groups at each time point is included at the bottom of the graph. (**C**) Vascular density is reduced in the lungs of *Ido1*$^{-/-}$ mice. Lung tissue sections from 5 WT and 5 *Ido1*$^{-/-}$ mice were stained with anti-caveolin-1 antibody to visualize blood vessels by immunofluorescence. Four images per tissue section were acquired and area measurements of every blood vessel within each field were recorded using AxioVision Release 4.6 software. All of the area measurements were tallied and plotted sequentially in ascending order from smallest to largest with vessel areas graphed on a log scale. As delineated in the segregated presentation of these data in Fig. 2E, the differential in vessel density apparent from this graph is due almost entirely to a reduced number of medium to small sized vessels in the lungs of *Ido1*$^{-/-}$ mice while the number of large vessels (>5,000 μm^2) is nearly the same as in the WT mice.

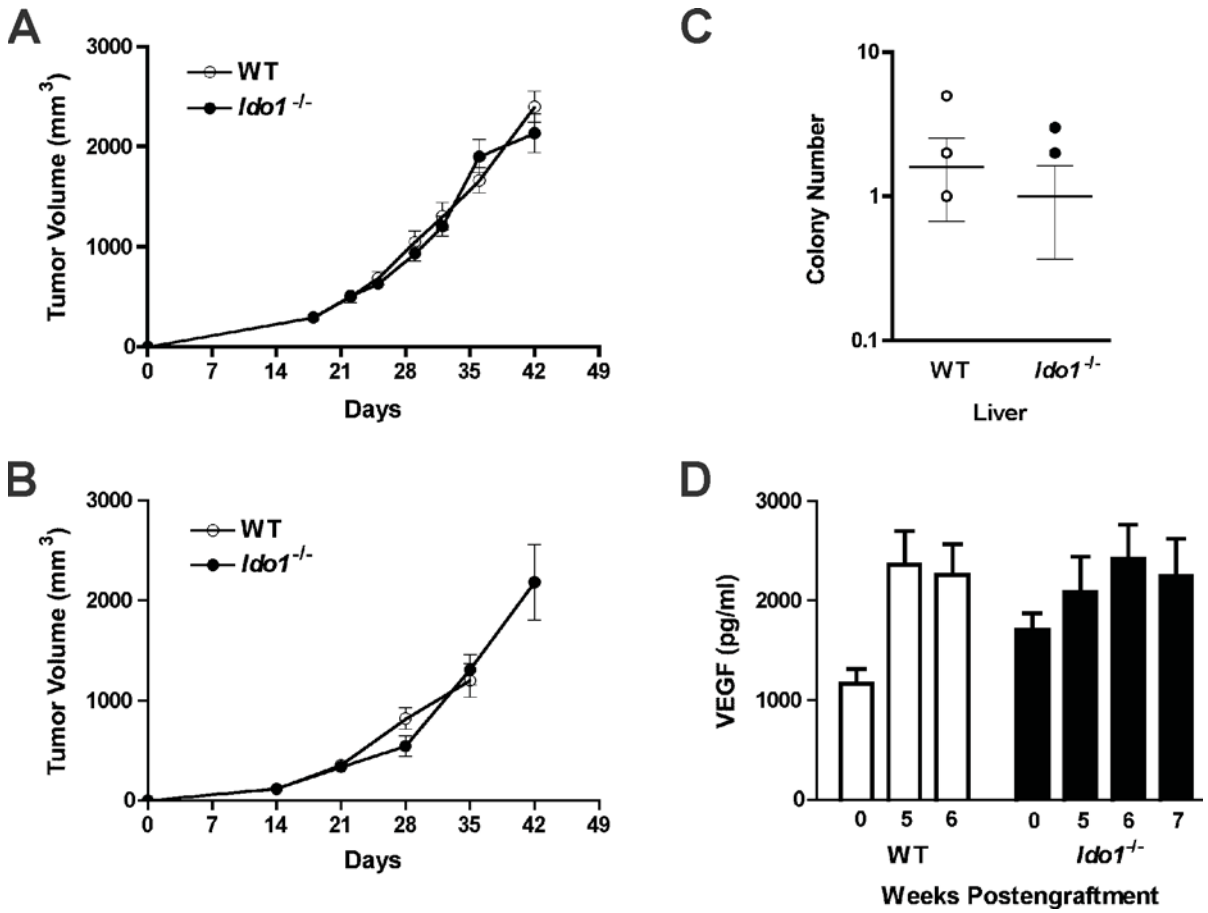

Supplementary Figure S2. (**A,B**) Primary 4T1 tumor growth is unaffected in *Ido1*$^{-/-}$ mice. WT and *Ido1*$^{-/-}$ mice received orthotopic grafts of (**A)** 4T1-luc (*N* = 20) or (**B**) 4T1 (*N* = 5) cells. Beginning at approximately 14 days, when a palpable tumor mass had become apparent, caliper measurements were made on a weekly basis to calculate primary tumor volumes. The data are plotted as means ± SE. Measurements for WT mice challenged with 4T1 cells at 42 days were not collected due to metastasis-associated mortality in this group. (**C**) *Ido1*$^{-/-}$ mice exhibit no demonstrable resistance to 4T1 liver metastasis formation. At 6 weeks following orthotopic injection of 4T1-luc cells into WT and *Ido1*$^{-/-}$ hosts (*N* = 5 per group), colony forming assays were performed to assess the relative tumor cell burden in the liver. Individual data points are graphed as a scatter plot on a log scale together with the means ± SE. Because the data are plotted on a log scale, points with a value of 0 are not represented in the scatter plot

but were included in computing the means. (**D**) VEGF is induced to similar levels in WT and *Ido1*$^{-/-}$ mouse lungs in response to 4T1 metastases. Mouse VEGF analysis was performed by the University of Maryland Cytokine Core Laboratory. Measurements of VEGF levels in homogenized lung samples from WT and *Ido1*$^{-/-}$ mice following orthotopic engraftment of 4T1 tumor cells at the time points in weeks indicted for each lane were assessed by two-antibody ELISA using biotin-streptavidin-peroxidase detection and are graphed as the means ± SEM ($N \geq 4$).

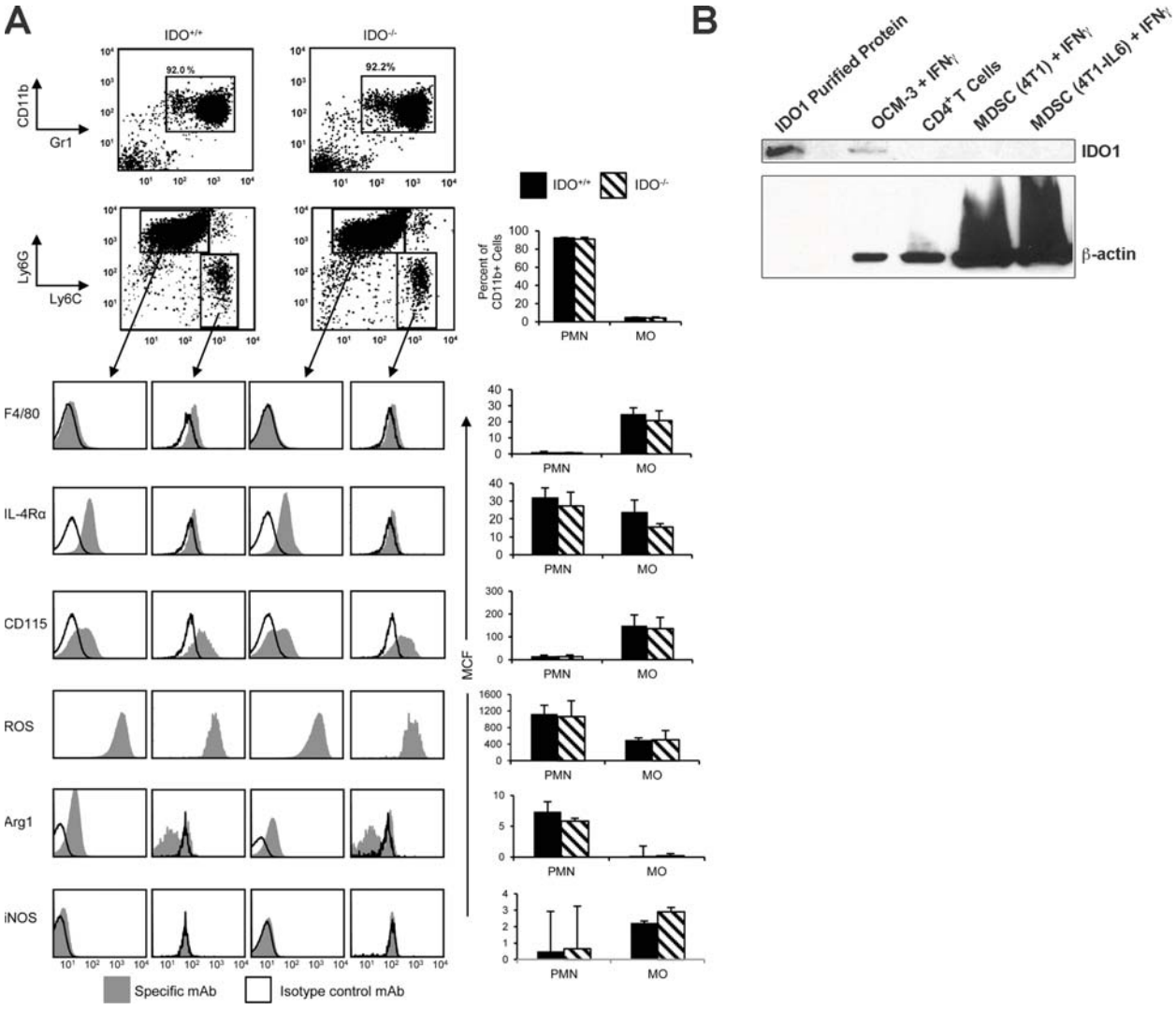

Supplementary Figure S3. (**A**) Phenotypic characterization reveals no demonstrable differences between MDSCs from WT and *Ido1*$^{-/-}$ mice. BALB/c strain WT and *Ido1*$^{-/-}$ mice were inoculated in the abdominal mammary gland with 10^5 4T1 mammary carcinoma cells. MDSC were harvested from the blood when WT and *Ido1*$^{-/-}$ mice had primary tumors that were not significantly different in size (12.2 ± 1.36 and 11.5 ± 0.4 mm in diameter, respectively). Red blood cells were removed by lysis and the remaining leukocytes were stained with mAbs to Gr1 and CD11b, or with mAbs to CD11b, Ly6C, Ly6G, and either arginase I, iNOS, CD115, F4/80, IL-4Rα and their respective isotype control mAbs, or with DCFDA to detect ROS. Gated CD11b$^+$

cells were analyzed for Ly6C and/or Ly6G expression. Granulocytic (PMN) and monocytic (MO) MDSC were identified as per Youn et al. (J. Immunol. 2008, 18:5791-802) as $CD11b^{+}Ly6G^{+}Ly6C^{-}$ or $CD11b^{+}Ly6G^{-}$ $Ly6C^{+}$ cells, respectively. Flow cytometry dotplots and histograms show MDSC from representative individual mice; graphs depict the average percent $Gr1^{+}CD11b^{+}$ cells or average mean channel fluorescence (MCF) for three mice per group. The values for total MDSC ($Gr1^{+}CD11b^{+}$) and for MO and PMN MDSC for iNOS, arginase, CD115, F4/80, IL-4Rα, and ROS are not statistically significantly different between MDSC from WT and *Ido1*$^{-/-}$ mice (Student's two-tailed *t* test with equal variance). (**B**) MDSCs from 4T1 tumor bearing mice lack detectable IDO1 expression. Western blot analysis using antibodies to IDO1 (top panel) and β-actin (bottom panel; loading control) with each lane individually labeled at the top. (Lanes 1,2) purified IDO1 protein for size confirmation with the adjacent lane left blank to avoid spillover contamination, (Lane 3; positive control) IFNγ-induced expression of IDO1 in OCM-3, a human melanoma cell line, (Lane 4; negative control) CD4 T cells lacking IDO1 expression, (Lane 5,6; experimental) MDSC isolated from 4T1 or 4T1-IL6 tumor-bearing mice and stimulated with IFNγ for 24 hours prior to analysis.